CHAPTER IV
RESULTS AND DISCUSSION

4.1 Kinetic Study of the PS/NR Reactive Blending

4.1.1 Rate of Reaction

The reaction rate of PS/NR blends using DCP as free radical initiator was determined by the slope of the plot of reaction torque versus reaction time (dTorque/dt). The DCP amount in the blends was varied as 0.5, 1.0, 1.5, and 2.0 phr. It was clearly seen that when there is no DCP, torque reduced with time revealing that the blend viscosity reduced probable due to shear thinning effect and mechanical degradation of polymer chains. When DCP was added, the dTorque/dt value was found to increase with increasing DCP amount shown in Table 4.1. So, the reaction rate in [PS/NR]/DCP blend system increased as amount of initiator increased.

Table 4.1 The dTorque/dt value of PS/NR reactive blending at initial stage of blending after DCP addition.

Blend compositions	dTorque/dt (Nm/s)
[PS/NR]/DCP, [60/40]/0	-0.0283
[PS/NR]/DCP, [60/40]/0.5	0.0386
[PS/NR]/DCP, [60/40]/1.0	0.0550
[PS/NR]/DCP, [60/40]/1.5	0.0786
[PS/NR]/DCP, [60/40]/2.0	0.1300

4.2 Characterization of the PS/NR Reactive Blend

In PS/NR melt blending process using DCP as an initiator, many kinds of end products were produced in free radical reaction system, e.g.,

crossslinked NR, a copolymer of PS and NR, PS and NR short chains. Thermal properties of the blends were observed by differential scanning calorimeter. The gel content and PS part of the blends with variation of DCP content were determined by dissolving in toluene and MEK and filtering. Moreover, the PS part dissolved in MEK were detected by FT-IR.

4.2.1 Determination of Gel Content

Gel content of PS/NR blends at various DCP contents: 0, 0.5, 1.0, 1.5, and 2 phr were shown in Figure 4.1. The gel content increased as the amount of DCP increased. Degree of gelation was not generated over 40 %wt corresponding to content of NR part.

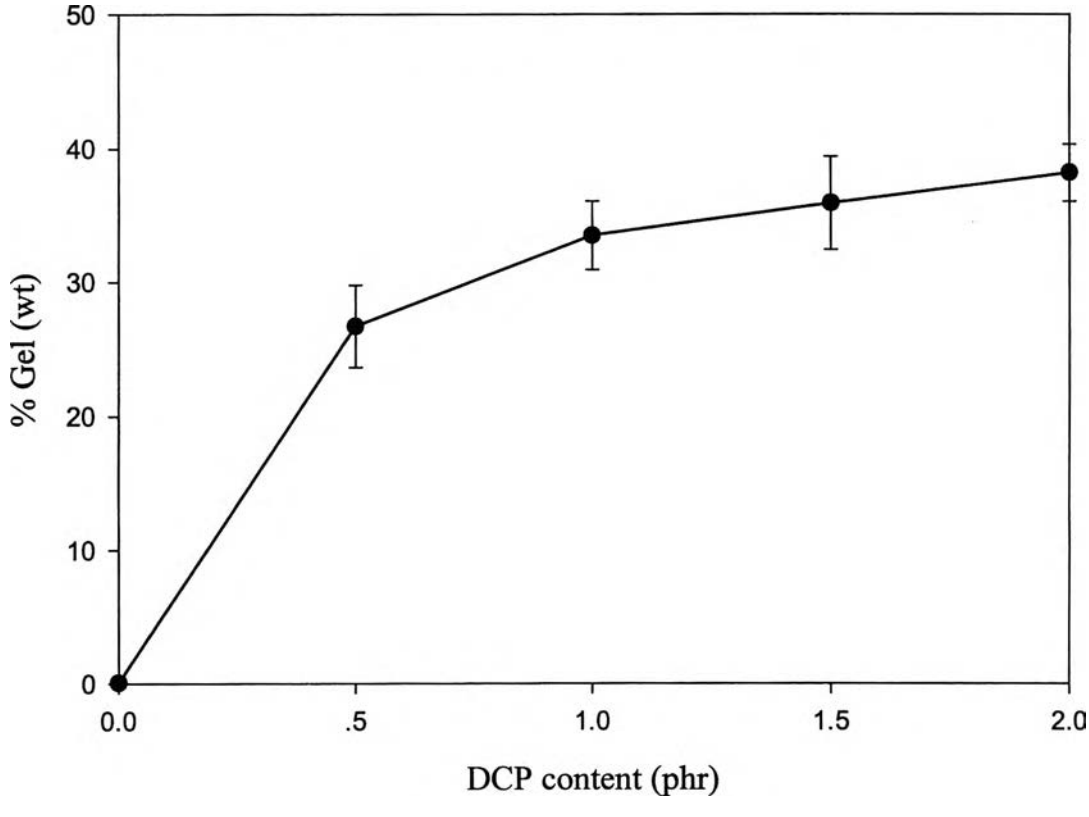

Figure 4.1 Effect of DCP content on gel content of PS/NR blends.

4.2.2 Determination of PS Part

The PS part was determined from the evaporated filtrate part (no gel) from MEK dissolution step at various DCP content (0-2phr). The result was shown in Figure 4.2 that %PS increased as content of DCP increased. %PS went up to 100 %wt for DCP content of 1.5 and 2.0 phr respectively. Both results imply that the reaction of DCP to NR and PS were likely to cause crosslinking in NR phase rather than reaction in PS phase. This brought about the increase in torque. However, it was possible that at low DCP contents, reaction between NR and PS could occur. So, the PS-NR blend with DCP 0.5 phr was used as compatibilizer in [Nylon12/NR]/ Compatibilizer.

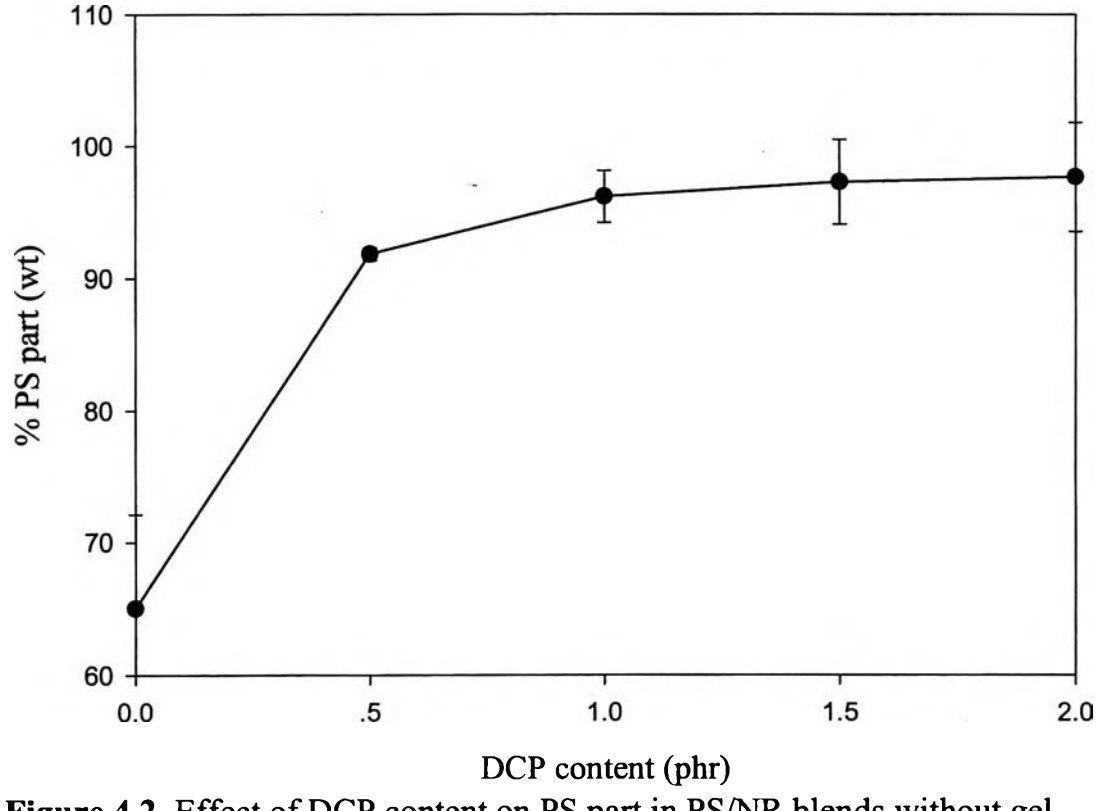

Figure 4.2 Effect of DCP content on PS part in PS/NR blends without gel.

The purposed reaction between PS and NR with DCP was shown in figure 4.3.

a) Initiation

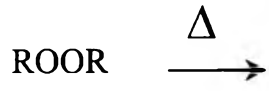

ROOR → 2RO• [1]

(DCP)

b) Propagation

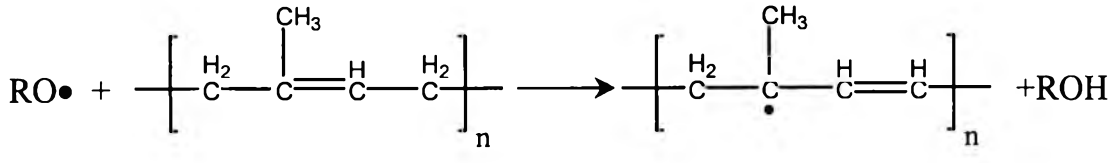

RO• + (NR) → (A) + ROH [2]

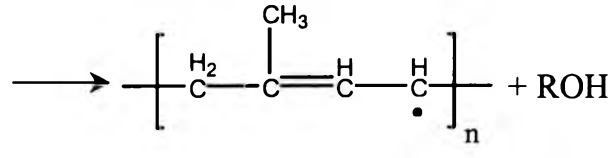

→ (B) + ROH [3]

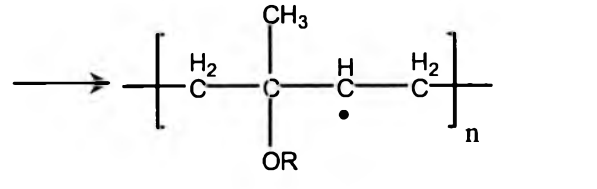

→ (C) [4]

RO• + (PS) → (D) + ROH [5]

c) Termination

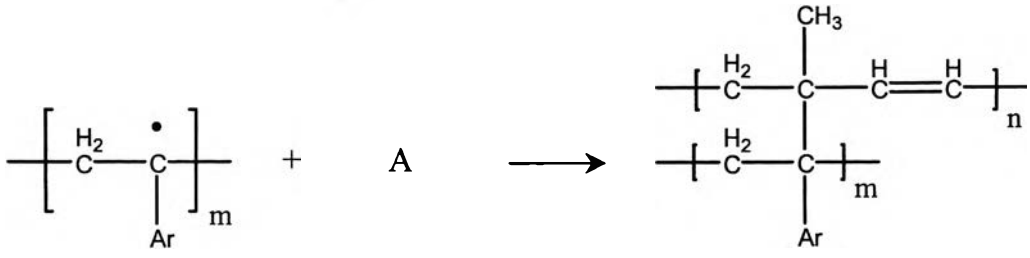

[6]

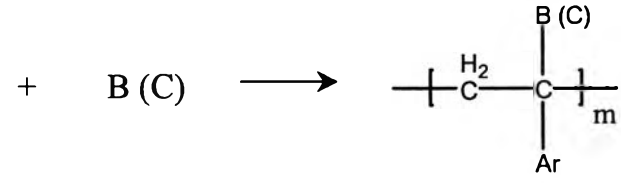

[7]

Figure 4.3 The proposed reaction between PS and NR with DCP by melt blending.

4.2.3 Thermal Properties of PS/NR Blends

Glass temperatures (T_g) of the crude blends were determined by DSC. T_g of PS in the blends decreased with increasing DCP content shown in Figure 4.4. Thus suggests that there was the linkage between rubber and PS molecule, thus PS became plashed by the rubber. These results also revealed that, at high DCP content, although the reaction between NR and PS was less predominant and gel content was high, there was a large total conversion to compatibilize. However, to avoid too high gel content, which might affected the long-term mechanical properties, DCP content of 0.5 phr was used to prepare the reaction blending of PS and NR for further use as compatibilizer in a Nylon12/NR blend.

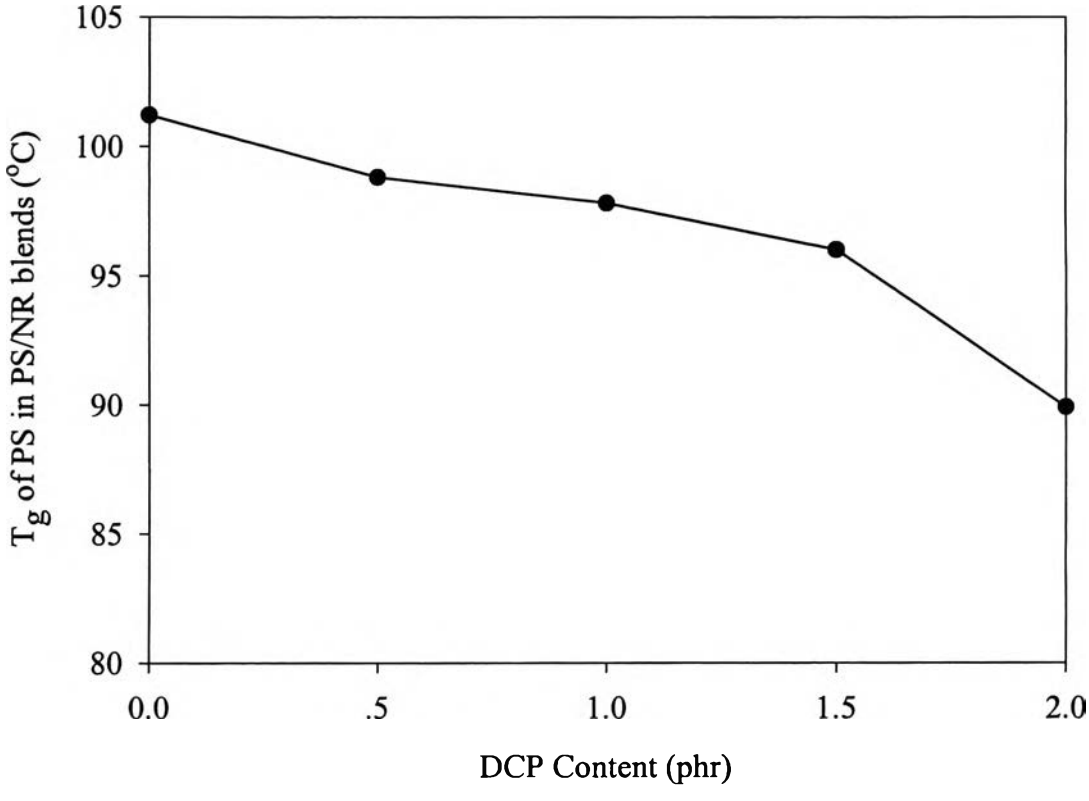

Figure 4.4 T_g of PS in PS/NR blends with variation of DCP content.

4.2.4 FT-IR Results of [PS/NR] Blend

The PS part of the blends that was dissolved by MEK were determined by FT-IR spectroscopy. The spectrum in Figure 4.5 from PS part of PS/NR blend with DCP 0.5 phr showed an absorbance peak at 843 cm^{-1} that is characteristic of ternary double bond in natural rubber. In NR spectrum, it also showed the little presence of protein by showing N-H stretching at around 3060 cm^{-1} and C=O stretching at 1640 cm^{-1}.

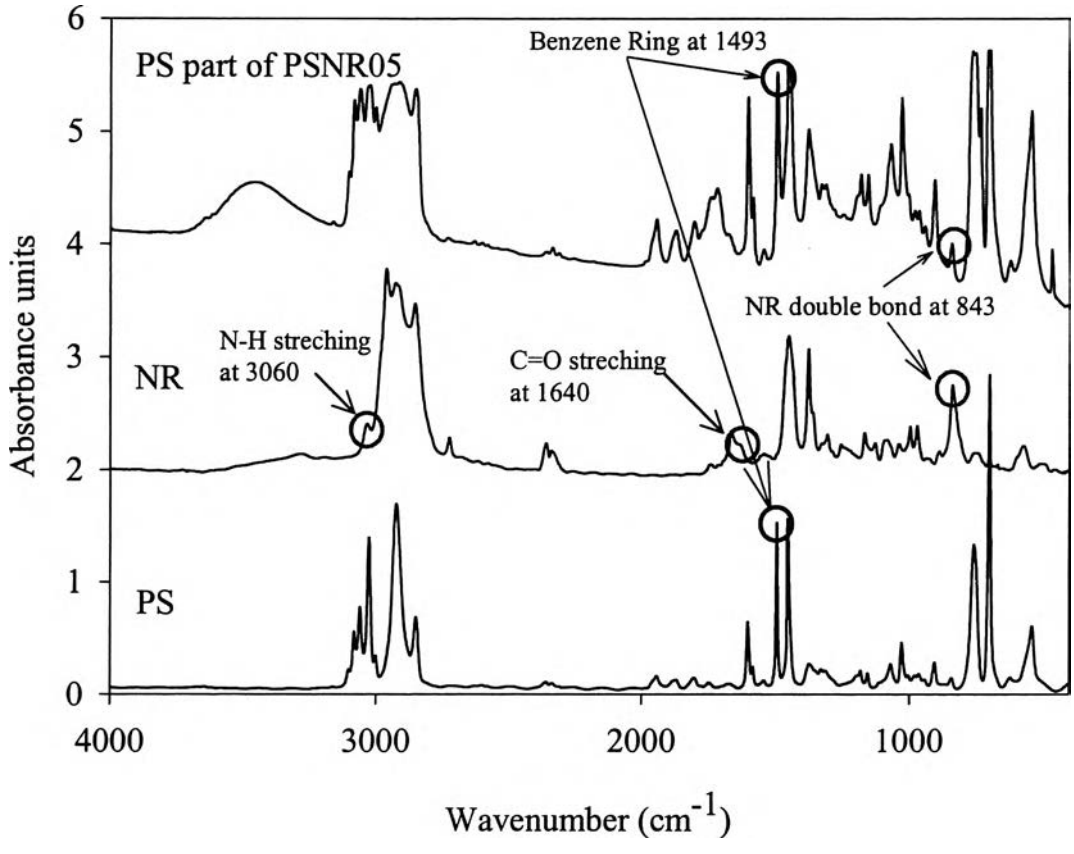

Figure 4.5 FT-IR spectra of PS part from PS/NR blend with DCP 0.5 phr, pure PS, and pure NR.

4.3 [Nylon12/NR]/Compatibilizer Characterization

4.3.1 Determination Exothermic or Endothermic Reaction of Ternary Blends

The determination of exothermic or endothermic character in [Nylon12/NR]/compatibilizer blend systems was taken as the time derivative of the temperature (dT/dt) from temperature profile after addition of the compatibilizer. The (dT/dt) value versus compatibilizer content was shown in Figure 4.6. The [Nylon12/NR]/G1652 blend systems showed that dT/dt values slightly increased with increasing SEBS G1652 content because the

elastomer fraction of the blend increased so the viscous heat was increase. In the reactive blending system, [Nylon12/NR]/FG1901x blends showed a larger increase in (dT/dt) values at high compatibilizer content because amine end groups of Nylon12 reacted well with maleic anhydride functional group of SEBS-g-MA compatibilizer and the reaction dissipated heat to the system, i.e. exothermic reaction. Moreover , the larger molecules induced by the reach between Nylon12 and SEBS-g-MA also generated more viscous heat.

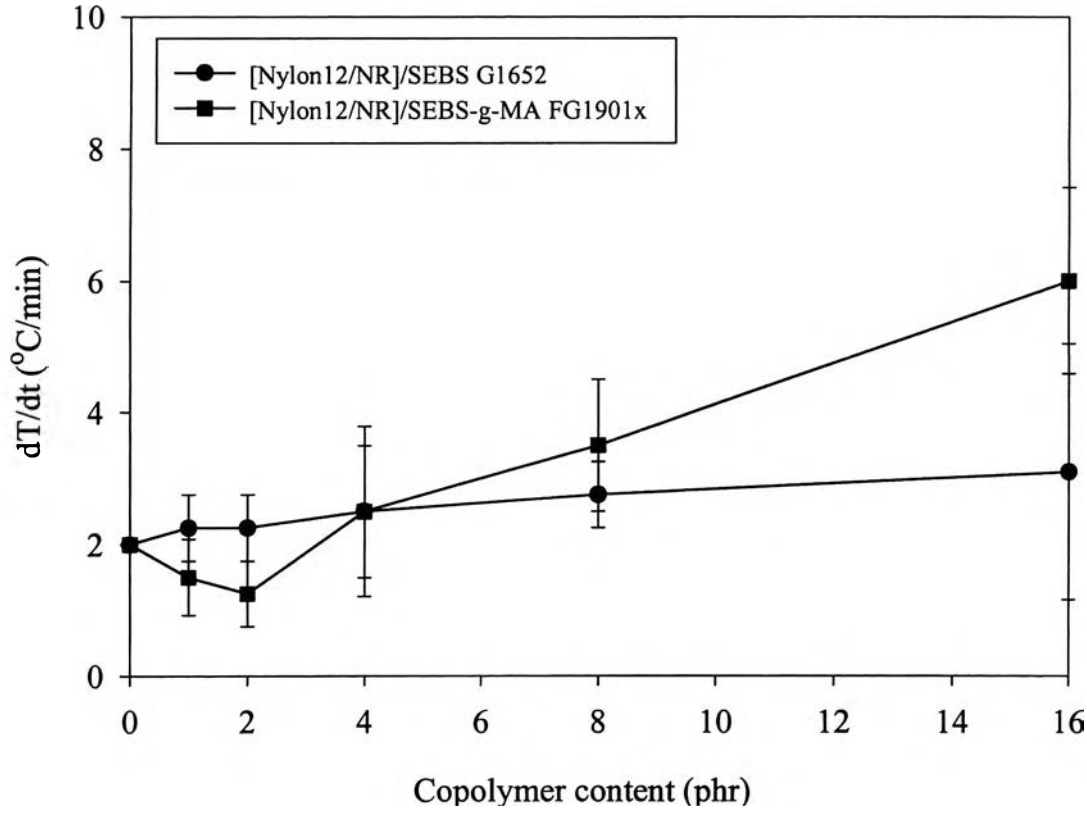

Figure 4.6 Effect of compatibilizer types and content on (dT/dt) value of [Nylon12/NR]/G1652 and [Nylon12/NR]/FG1901x systems at the initial stage of mixing.

4.3.2 Morphology Prediction by Interfacial Tension

In order to predict phase morphology from the interfacial tension between the blend components, the value of γ_{12}, γ_{32}, and γ_{13} have been estimated by harmonic mean equation at the mixing temperature (190°C)

$$\gamma_{12} = \gamma_1 + \gamma_2 - \frac{4\gamma_1^d \gamma_2^d}{\gamma_1^d + \gamma_2^d} - \frac{4\gamma_1^p \gamma_2^p}{\gamma_1^p + \gamma_2^p} \tag{4.1}$$

where the superscripts d and p refer to the dispersive and polar contributions of the surface tension γ, respectively. Thus, data for the polarities (γ^p/γ) and the changing in surface tension with temperature (dγ/dT) were required to complete surface tension value. The spreading coefficient was calculated by Harkin's equation from interfacial tension data. The interfacial tensions and spreading coefficient were listed in Table 4.1. The change in surface tension with temperature (dγ/dT) of Nylon 12 was assumed to be the same as for Nylon10,10 (Van Krevelan, 1990, ch.4, 7 and 8). The NR data was assumed to be the same as for cis-polyisoprene (Wu, 1989, ch.6). No polarity (x^p) and dγ/dT value for polyisoprene was available. The x^p was calculated from

$$\frac{\gamma^p}{\gamma} = \frac{\delta^p}{\delta}^2 \tag{4.2}$$

where δ and δ^p are the polyisoprene solubility parameter and its polar component (Wu, 1989, ch.6). Since dγ/dT property lies in a narrow range (0.056-0.077), the NR surface tension has been calculated by using these values for dγ/dT of NR, i.e. 0.055, 0.065, and 0.075 (Luzinov, 1999). PS data were available in the scientific literatures (Wu, 1989, ch.6). In the case of SEBS copolymer, the calculations were done separately for the styrene part and ethylene butylene part. The ethylene butylene surface tension was assumed to be the same as poly(ethylene-stat-polypropylene) (Wu, 1989, ch.6). Values for γ, γ^p, and γ^d at 190°C have been calculated see Table 4.2.

Table 4.2 Estimated surface tension of polymers at the processing temperature (190°C).

Polymer	γ at 20°C (mN/m)	Polarity	$-d\gamma/dT$ (mN/m°C)	γ at 190°C (mN/m)		
				γ	γ^d	γ^p
Nylon12	35.8	0.154	0.065	24.75	20.94	3.81
NR ($-d\gamma/dT = 0.055$)	32.0	0.030	0.055	22.65	21.97	0.68
NR ($-d\gamma/dT = 0.065$)			0.065	20.95	20.32	0.63
NR ($-d\gamma/dT = 0.075$)			0.075	19.25	18.67	0.58
PS	40.7	0.168	0.072	28.46	23.68	4.78
EB	31.0	0.000	0.058	21.14	21.14	0.00

The interfacial tension values calculating by harmonic mean equation from equation 4.2 list in Table 4.3. The interfacial tension between Nylon12 and PS showed lower interfacial tension than between Nylon12 and EB so SEBS should have the PS block facing to the Nylon part. For the NR/SEBS pair, the interfacial tension between NR and PS were showed much higher interfacial tension than between NR and EB so SEBS tended to face EB block to the NR surface. For PS/NR blend, PS part should faced to Nylon12 surface and NR part faced to NR phase.

Table 4.3 The calculation of interfacial tension values of polymers at the processing temperature (190°C).

Polymer Pairs	γ_1 (mN/m)	γ_2 (mN/m)	γ^d_1 (mN/m)	γ^p_1 (mN/m)	γ^d_2 (mN/m)	γ^p_2 (mN/m)	γ_{12} (mN/m)
Nylon12/NR (-dγ/dT = 0.055)	24.75	22.65	20.94	3.81	21.97	0.68	2.21
Nylon12/NR (-dγ/dT = 0.065)	24.75	20.95	20.94	3.81	20.32	0.63	2.29
Nylon12/NR (-dγ/dT = 0.075)	24.75	19.25	20.94	3.81	18.67	0.58	2.51
Nylon12/PS	24.75	28.46	20.94	3.81	23.68	4.78	0.28
Nylon12/EB	24.75	21.14	20.94	3.81	21.14	0.00	3.81
NR (-dγ/dT = 0.055)/PS	22.65	28.46	21.97	0.68	23.68	4.78	3.14
NR (-dγ/dT = 0.065)/PS	20.95	28.46	20.32	0.63	23.68	4.78	3.44
NR (-dγ/dT = 0.075)/PS	19.25	28.46	18.67	0.58	23.68	4.78	3.89
NR (-dγ/dT = 0.055)/EB	22.65	21.14	21.97	0.68	21.14	0.00	0.70
NR (-dγ/dT = 0.065)/EB	20.95	21.14	20.32	0.63	21.14	0.00	0.65
NR (-dγ/dT = 0.075)/EB	19.25	21.14	18.67	0.58	21.14	0.00	0.73

The spreading coeffcient values were calculated by Harkin's equation (1.2). The interfacial tension between Nylon12 and SEBS G1901x was assumed to be zero because amine end group of Nylon12 and maleic anhydride group of SEBS-g-MA could react together. The interfacial tension between NR and SEBS was assumed to use NR/EB value because of lower tension than NR/PS interface. In [Nylon12/NR]/SEBS system, the spreading coefficient values of NR on SEBS phase were negative but that of SEBS phase on NR phase was positive so it was predicted that SEBS would encapsulate NR phase in Nylon12 matrix. For [Nylon12/NR]/SEBS-g-MA system, the spreading coefficient value of SEBS-g-MA on NR phase was more positive than the spreading coefficient of [Nylon12/NR]/SEBS system so it is predicted that SEBS-g-MA would tend to encapsulate NR easier than SEBS shown in Table 4.4. In [Nylon12/NR]/[PS/NR blend], [PS/NR blend] should encapsulated NR readily because it showed the highest spreading coefficient.

Table 4.4 The calculation of the spreading coefficient values in ternary blends at the processing temperature (190°C).

Blends	Phase x on Phase y	γ_{12} (mN/m)	γ_{13} (mN/m)	γ_{23} (mN/m)	λ_{xy} (mN/m)
[Nylon12/NR]/SEBS	NR on SEBS	0.70	0.28	2.21	-2.63
(-dγ/dT of NR = 0.055)	SEBS on NR	0.70	2.21	0.28	1.24
[Nylon12/NR]/SEBS	NR on SEBS	0.65	0.28	2.29	-2.65
(-dγ/dT of NR = 0.065)	SEBS on NR	0.65	2.29	0.28	1.36
[Nylon12/NR]/SEBS	NR on SEBS	0.73	0.28	2.51	-2.96
(-dγ/dT of NR = 0.075)	SEBS on NR	0.73	2.51	0.28	1.50
[Nylon12/NR]/SEBS-g-MA	NR on SEBS-g-MA	0.70	0.00	2.21	-2.90
(-dγ/dT of NR = 0.055)	SEBS-g-MA on NR	0.70	2.21	0.00	1.51
[Nylon12/NR]/SEBS-g-MA	NR on SEBS-g-MA	0.65	0.00	2.29	-2.93
(-dγ/dT of NR = 0.065)	SEBS-g-MA on NR	0.65	2.29	0.00	1.64
[Nylon12/NR]/SEBS-g-MA	NR on SEBS-g-MA	0.73	0.00	2.51	-3.24
(-dγ/dT of NR = 0.075)	SEBS-g-MA on NR	0.73	2.51	0.00	1.78
[Nylon12/NR]/[PS/NR blend]	NR on [PS/NR blend]	0.00	0.28	2.21	-1.93
(-dγ/dT of NR = 0.055)	[PS/NR blend] on NR	0.00	2.21	0.28	1.93
[Nylon12/NR]/[PS/NR blend]	NR on [PS/NR blend]	0.00	0.28	2.29	-2.01
(-dγ/dT of NR = 0.065)	[PS/NR blend] on NR	0.00	2.29	0.28	2.01
[Nylon12/NR]/[PS/NR blend]	NR on [PS/NR blend]	0.00	0.28	2.51	-2.23
(-dγ/dT of NR = 0.075)	[PS/NR blend] on NR	0.00	2.51	0.28	2.23

4.3.3 Effect of SEBS in Nylon12/NR Blends

4.3.3.1 *Phase Morphology Characterization by TEM*

The phase morphology of nylon12/NR blends was investigated by TEM after staining NR phase by OsO_4 to make phase contrast in the blends, see Figure 4.7(a). The [Nylon12/NR]/SEBS blend has the core-shell morphology with a wide dispersed phase size distribution. The SEBS phase (not stained by OsO_4) formed the core and was encapsulated by NR phase shown in Figure 4.7(b). This morphology did not follow the prediction based on interfacial tension that SEBS phase should remain at Nylon12/NR interface and encapsulates NR domains; i.e. PS block facing to Nylon12 phase, and EB block facing to NR phase. This may occurred because of using NR polarity data from synthetic cis-polyisoprene that were different from the polarity of NR because NR has a higher polarity groups from protein residues and from aldehyde, ketone, carboxylic acid and ester groups as known by NR thermal degradation (Li, 1999). So, the polarity of protein (0.2) was used and the interfacial tension data was changed see Table 4.5.

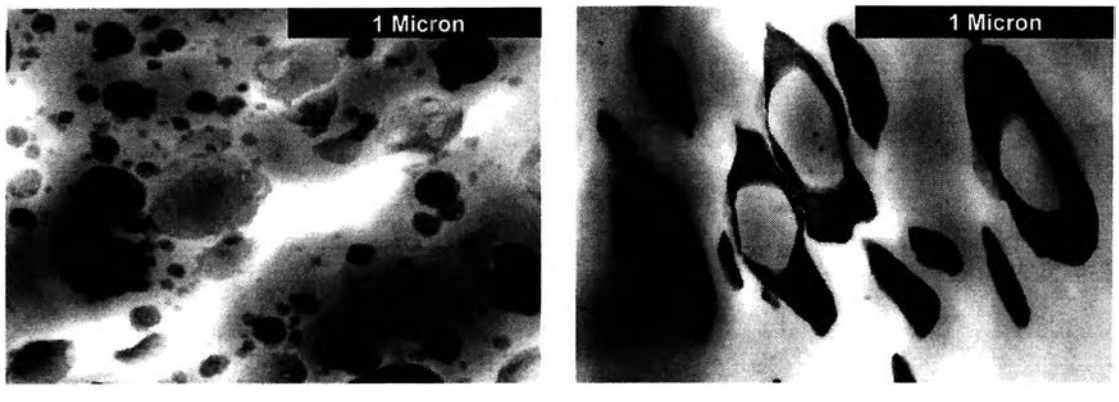

(a) (b)

Figure 4.7 TEM micrographs with a magnification of 55500x of the ultra thin microtomed (a) 80/20 Nylon12/NR blend and (b) the same blend with 4 phr of SEBS G1652.

Table 4.5 The new calculation of interfacial tension values of polymers at the processing temperature (190°C).

Polymer Pairs	γ_1 (mN/m)	γ_2 (mN/m)	γ^d_1 (mN/m)	γ^p_1 (mN/m)	γ^d_2 (mN/m)	γ^p_2 (mN/m)	γ_{12} (mN/m)
Nylon12/NR	24.75	22.65	20.939	3.812	18.12	4.53	0.264
Nylon12/PS	24.75	28.46	20.939	3.812	23.68	4.78	0.276
Nylon12/EB	24.75	21.14	20.939	3.812	21.14	0.00	3.812
NR/PS	22.65	28.46	18.12	4.53	23.68	4.78	0.746
NR/EB	22.65	21.14	18.12	4.53	21.14	0.00	4.762

4.3.3.2 *The Calculated Interfacial Thickness*

The interfacial thicknesses calculated by Equation 2.4 shown in table 4.6.

Table 4.6 The calculated interfacial thickness of polymers at the processing temperature (190°C).

Polymer Pairs	γ_{12} (mN/m)	Interfacial Thickness (nm)
Nylon12/NR	0.264	49.746
Nylon12/PS	0.276	47.240
Nylon12/EB	3.812	2.231
NR/PS	0.746	14.866
NR/EB	4.762	1.722

4.3.3.3 *Dispersed Phase Size Characterization by SEM*

The cryogenic fracture of the blends was observed by SEM after etching NR and SEBS phases by toluene (90%wt toluene/10%wt IPA for SEBS-g-MA). The dispersed phase size of [Nylon12/NR]/SEBS G1652 blends was increased as increasing the SEBS content see in Figures 4.8 and 4.9. The shape of the dispersed phase is irregular, and became more

spherical for the blends after addition of 1 phr SEBS. The number averages of dispersed phase size measurements were estimated by averaging the diameter of about 100 domains randomly for each blend system.

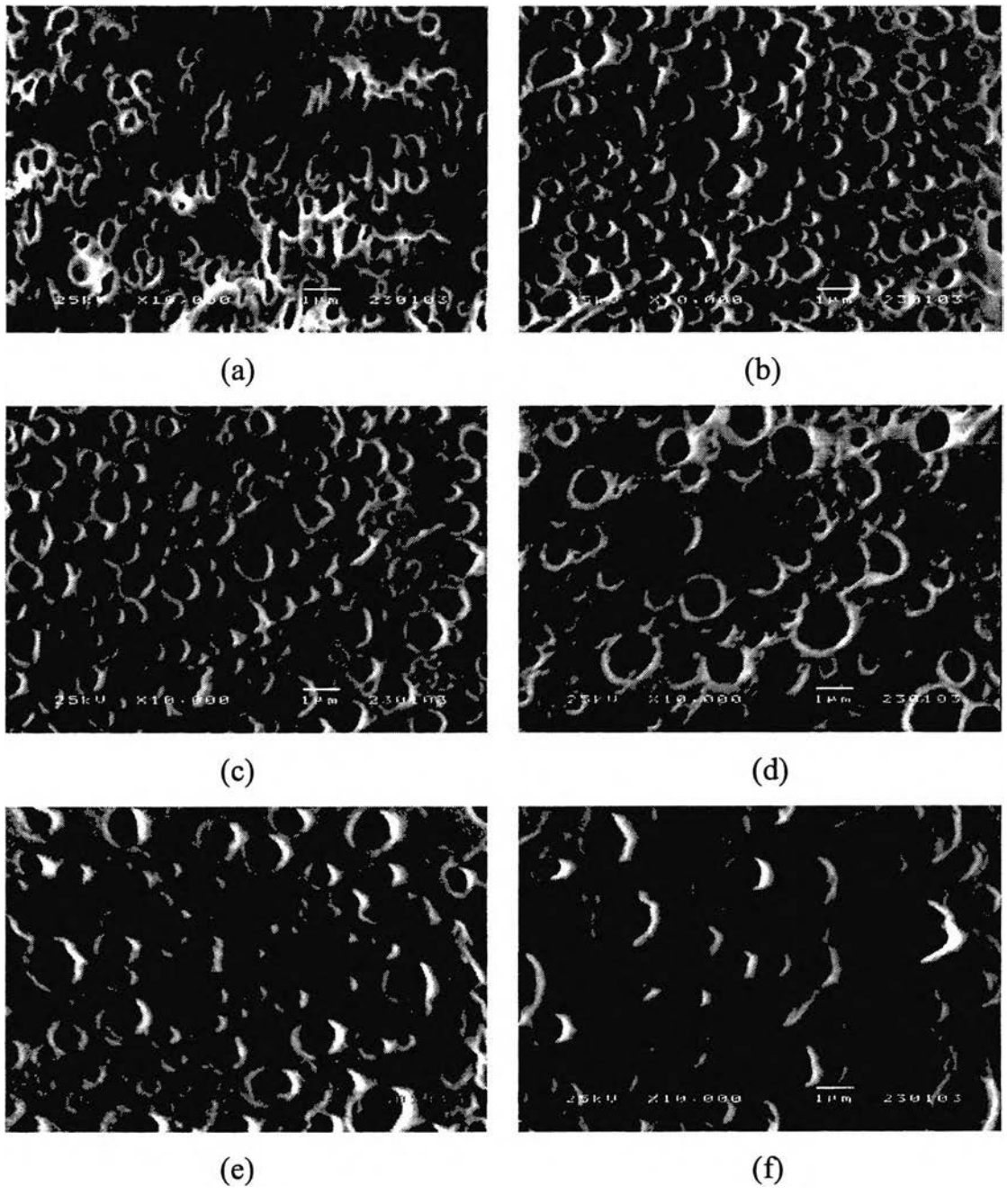

Figure 4.8 SEM micrographs of the cryofracture surfaces of the [80/20] [Nylon12/NR] blends at various SEBS G1652 content (a) 0 phr, (b) 1 phr, (c) 2 phr, (d) 4 phr, (e) 8 phr, and (f) 16 phr.

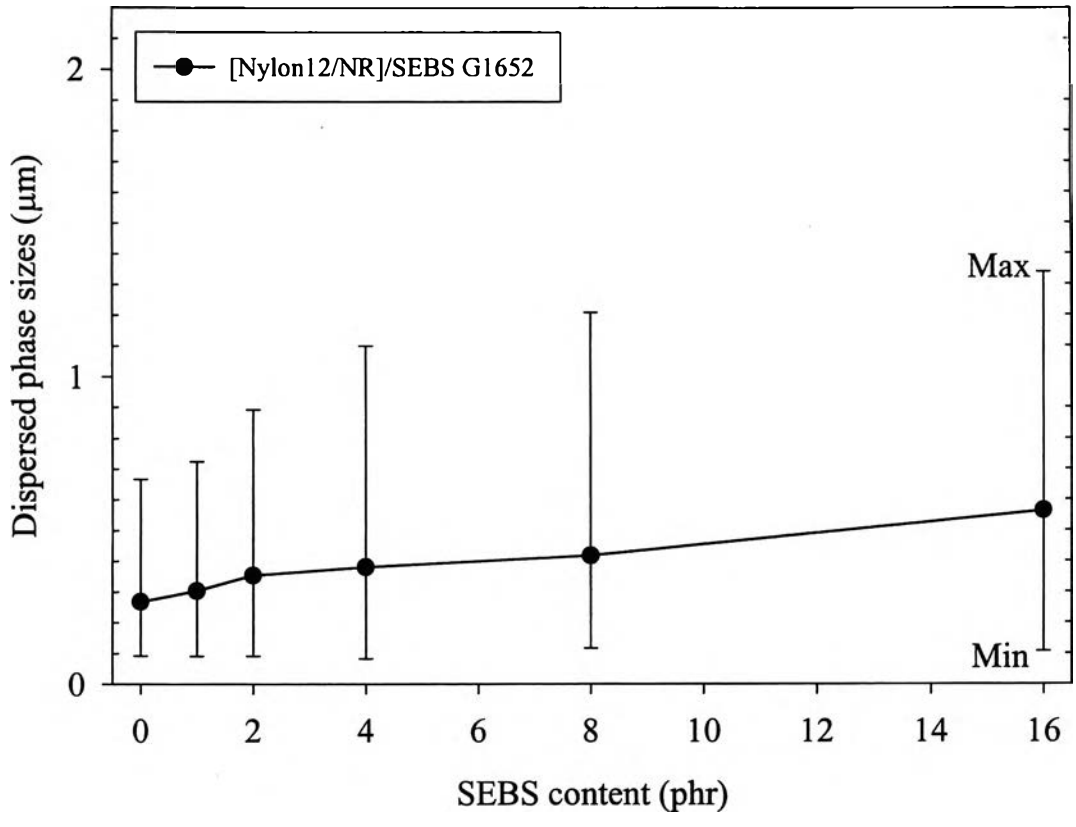

Figure 4.9 Dispersed phase size and distribution of [Nylon12/NR]/SEBS G1652 blends with 0, 1, 2, 4, 8, and 16 phr of SEBS.

4.3.3.4 *Mechanical Properties*

The effect of SEBS content on the tensile modulus was shown in Figure 4.10. With increase of the SEBS content in [Nylon12/NR] /SEBS G1652 blends, the tensile modulus increased initially then decreased continuously. At small content of SEBS, the increase of tensile modulus resulted from the suitable dispersed phase size, the strength of SEBS core, and effect of core-shell morphology. The lowering of tensile modulus was probably due to the coarser morphology because of the higher dispersed phase size in Nylon12 matrix implying that it had higher chance of coalescence due to the higher content of SEBS. Moreover, the lowering of the modulus came

from the lower %wt Nylon12 in blends. The morphology stabilization by this compatibilizer was not likely obtained.

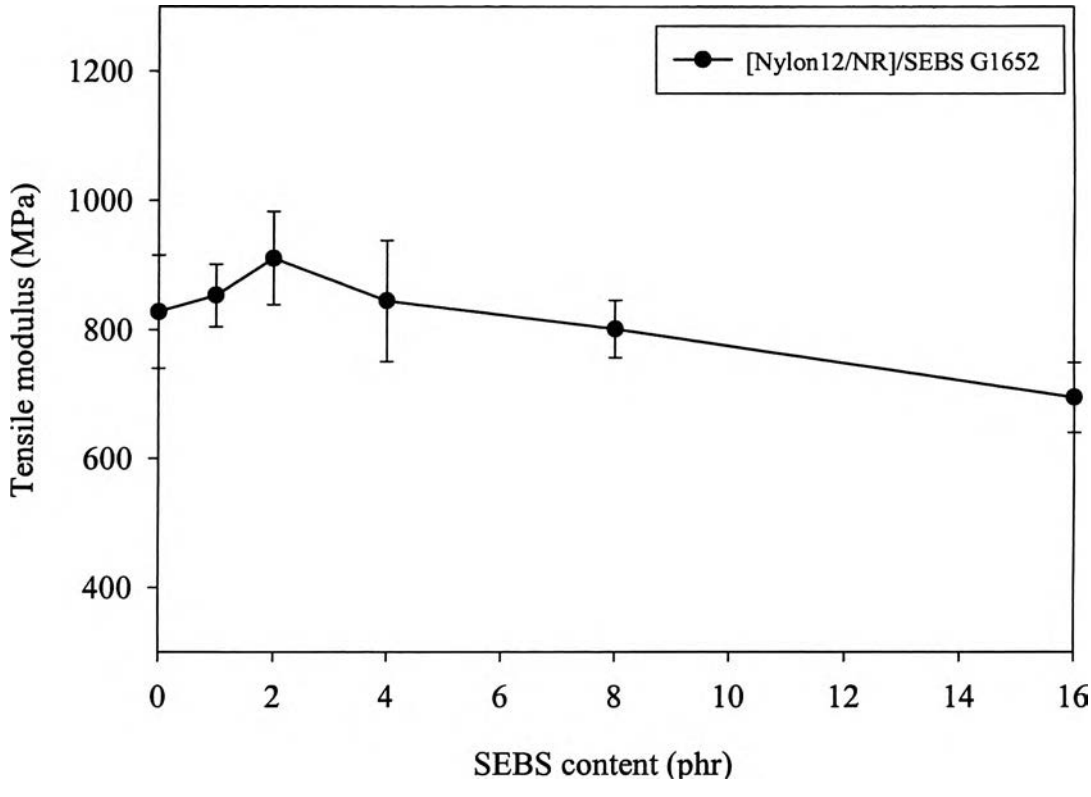

Figure 4.10 Effect of SEBS content on tensile modulus of [Nylon12/NR]/ SEBS G1652 blends with 0, 1, 2, 4, 8, and 16 phr of SEBS.

The effects of SEBS content on the tensile yield stress showed the same trend as tensile modulus see Figure 4.10. The tensile strength increased with small SEBS amount then decreased with increasing content of SEBS.

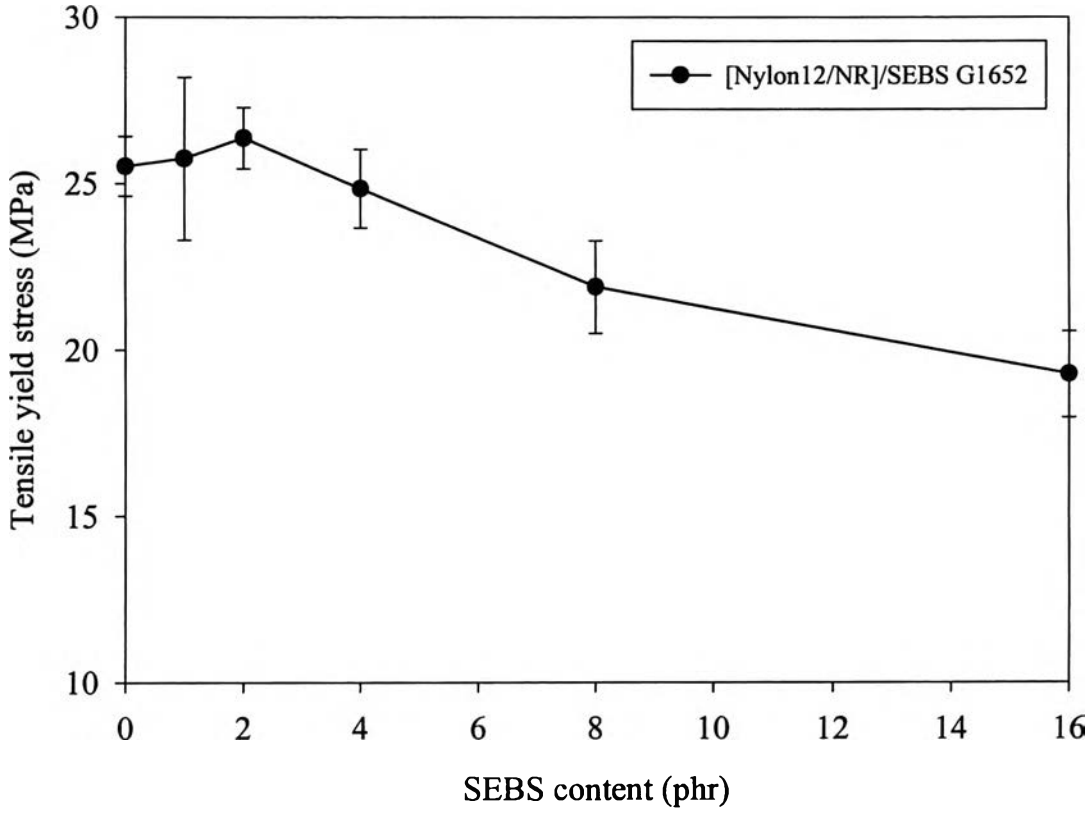

Figure 4.11 Effect of SEBS content on tensile yield stress of [Nylon12/ NR]/ SEBS G1652 blends with 0, 1, 2, 4, 8, and 16 phr of SEBS.

4.3.3.5 *Thermal Properties*

The [Nylon12/NR]/SEBS blends showed the leveling T_g, T_m, and T_c as increasing SEBS content see Figure 4.12. Thus, it was likely that SEBS hardly alters the blend structure and the decreasing mechanical strength results from some minor defect causing poor bulk cohesive strength; e.g. moderate phase adhesions and micelle formation of the compatibilizer.

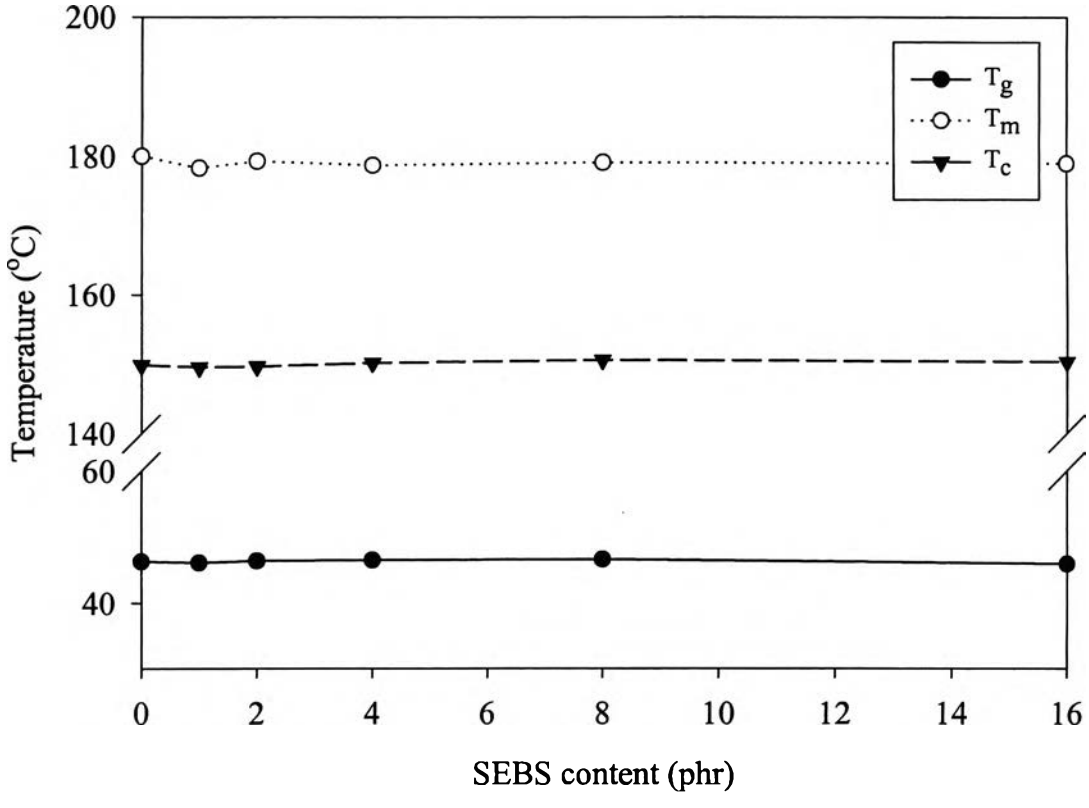

Figure 4.12 T_g, T_m, and T_c of Nylon12 in [Nylon12/NR]/SEBS blends with variation of SEBS content.

4.3.4 Effect of Reactive SEBS in Nylon12/NR Blends

4.3.4.1 *Phase Morphology Characterization by TEM*

The phase morphology of [Nylon12/NR]/SEBS FG1901x was the core-shell morphology. The NR phase was a core and encapsulated by the SEBS-g-MA phase. The 2%wt maleic anhydride on EB mid-block of SEBS G1901x reacted with amine end group of Nylon12 and reduced the interfacial tension between SEBS and Nylon12. So, There was no light stained core (SEBS-g-MA phase) with the dark droplet (NR phase) from TEM micrograph shown in Figure 4.13. This morphology was follows the interfacial tension prediction.

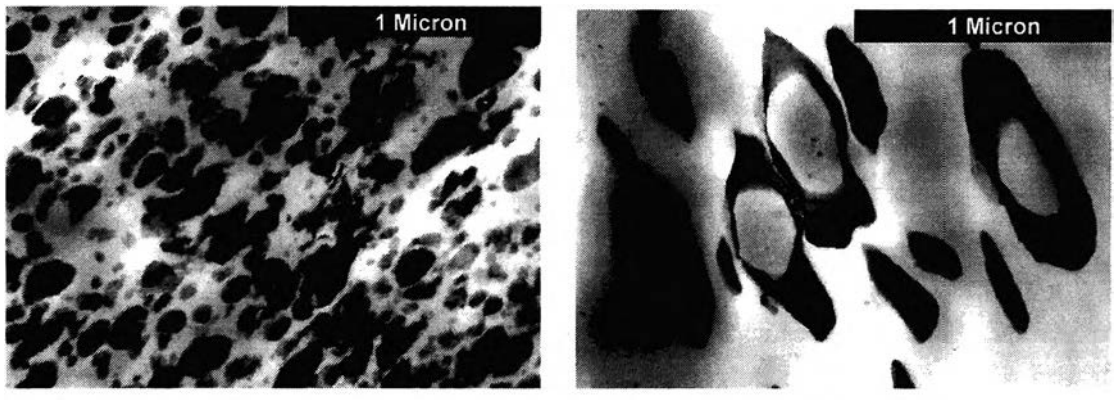

(a) (b)

Figure 4.13 TEM micrographs with a magnification of 55500x of the ultra thin microtomed (a) [80/20]/4phr [Nylon12/NR]/SEBS-g-MA FG1901x blend and (b) [80/20]/4phr [Nylon12/NR]/SEBS G1652 blend.

4.3.4.2 *Dispersed Phase Size Characterization by SEM*

The SEBS-g-MA-Nylon12 reaction product from the copolymer between SEBS-g-MA and Nylon12 act very efficiently as a compatibilizer. A reduction in dispersed phase size was occurred from the lowering of interfacial tension of Nylon12/NR interface shown in Figure 4.14. The average diameter decreased with increasing SEBS-g-MA content, the [Nylon12/NR]/SEBS-g-MA blend showed a reduction in disperse phase size and then levels off at the higher concentration see Figure 4.15. This leveling point could be considered as the interfacial saturation point where the concentration of SEBS-g-MA in [Nylon12/NR]/SEBS-g-MA was high enough to saturate the interface between Nylon12 and NR to produce perfect coreshell formation. The interfacial saturation point of this blend was about 2 phr of SEBS FG1901x. The morphology is then stabilized by reactive blending (the reaction prevents coalescence to occur).

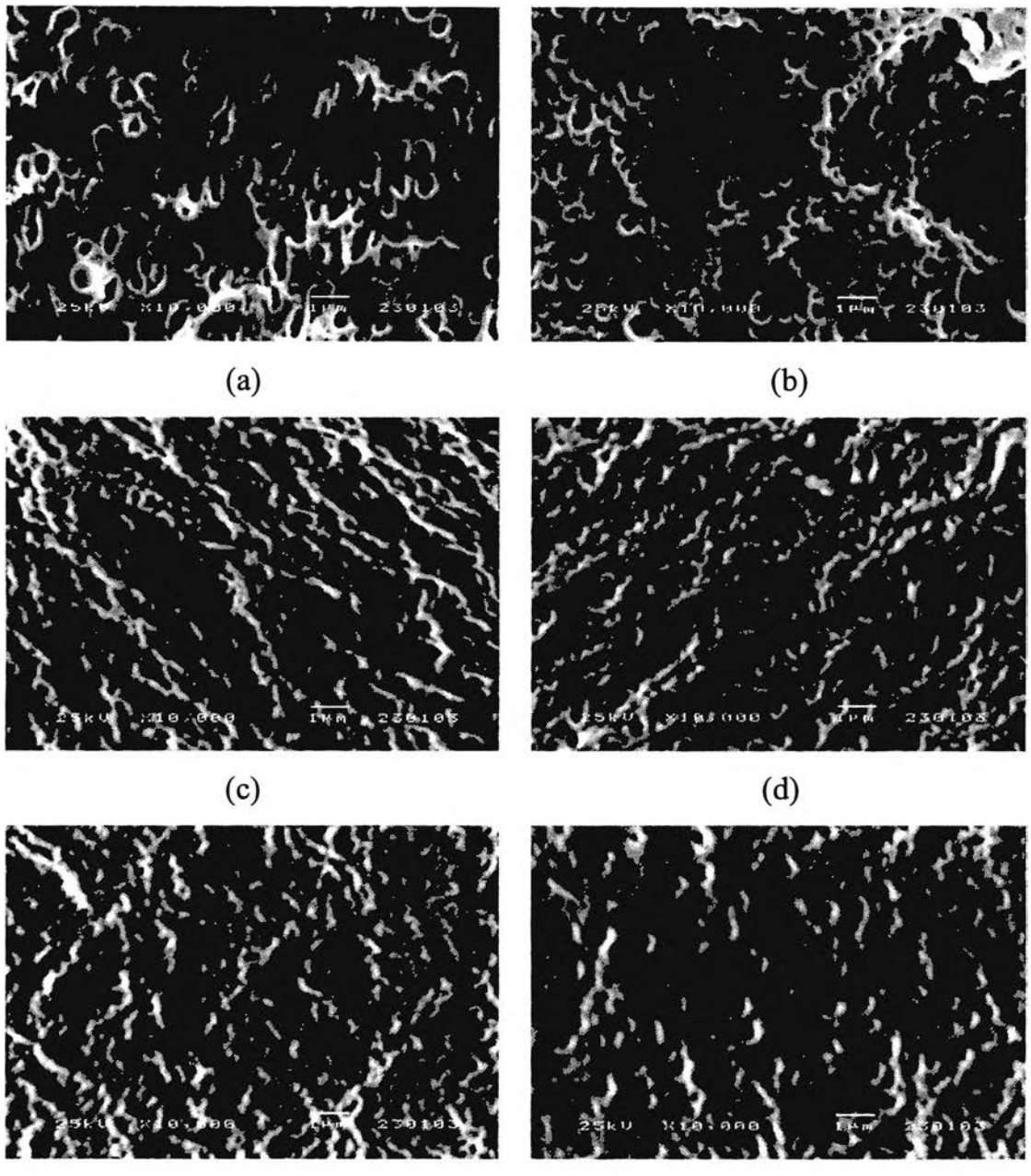

Figure 4.14 SEM micrographs of the cryofracture surfaces of the [80/20] [Nylon12/NR] blends at various SEBS-g-MA FG1901x contents (a) 0 phr, (b) 1 phr, (c) 2 phr, (d) 4 phr, (e) 8 phr, and (f) 16 phr.

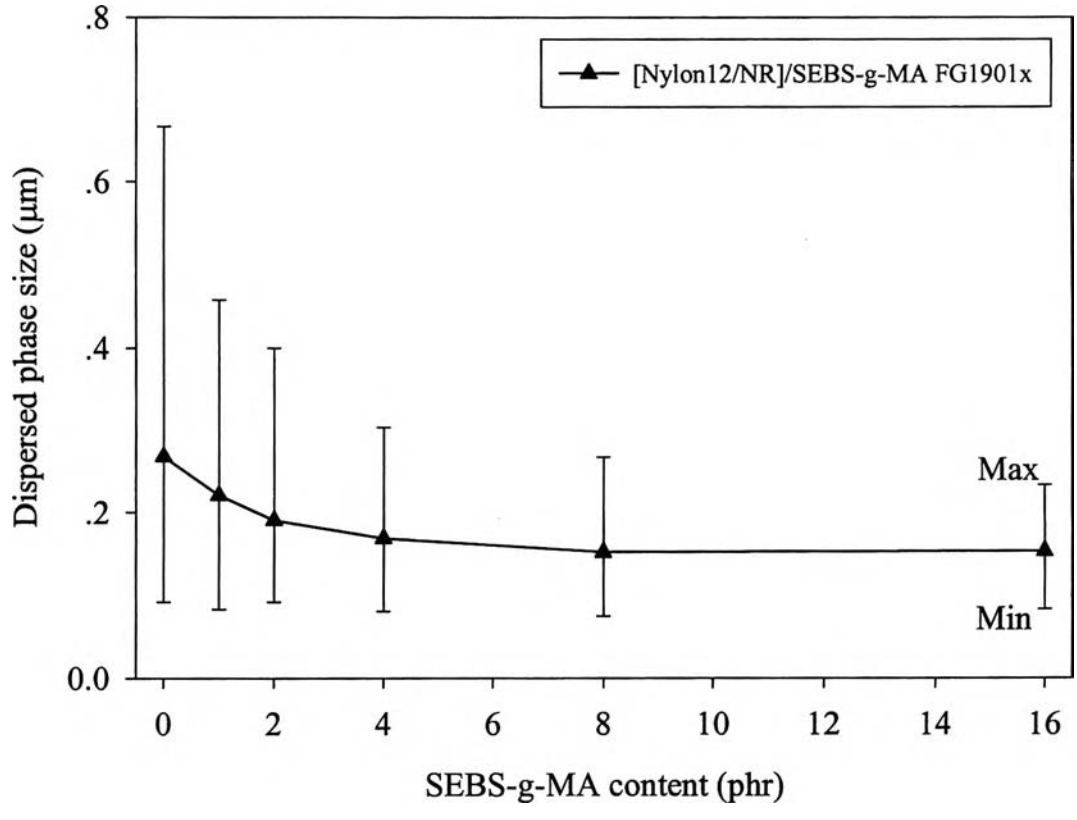

Figure 4.15 Dispersed phase size and distribution of [Nylon12/NR]/SEBS-g-MA FG1901x blends with 0, 1, 2, 4, 8, and 16 phr of SEBS-g-MA.

4.3.4.3 *Mechanical Properties*

The [Nylon12/NR]/SEBS-g-MA FG1901x (reactive blend) showed a higher tensile modulus than that of [Nylon12/NR]/SEBS G1652 (non-reactive) presumably due to better stress transfer between Nylon12 and SEBS-g-MA phase. However, the [Nylon12/NR]/SEBS-g-MA blend showed an increase of tensile modulus at small amount of SEBS-g-MA and then continuous decrease as in [Nylon12/NR]/SEBS blend. Since the MA part resides in EB block, increasing its content enhanced better adhesions to this soft phase and hence the modulus was lowered faster than the system with SEBS. However, this effect was not significant on tensile yield stress, which likely depended on crystalline structure. At small content of SEBS, the

increasing of tensile strength might occur from the higher interfacial adhesion between Nylon12 and SEBS, the strength of SEBS core, and effect of core-shell morphology. The lowering of tensile strength came from the micelle formation because the SEBS-g-MA content is higher than critical micelle concentration (CMC) (Asaletha, 1995) in the blend shown in Figure 4.16. Moreover, the lowering in the mechanical properties probably occurred from the decrease in crystallinity of Nylon as a result of extremely small thickness of Nylon interlayer due to physical hinderance (Van Duin, 1997).

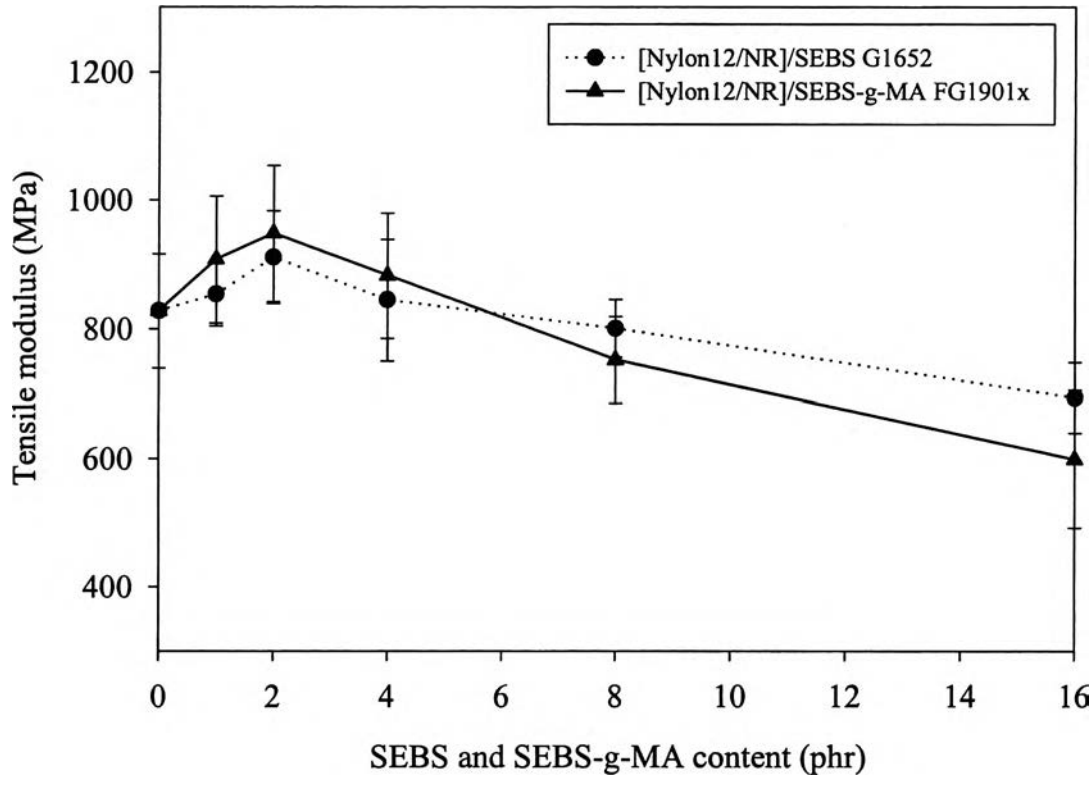

Figure 4.16 Comparison between effect of SEBS-g-MA and SEBS content on tensile modulus of 80/20 [Nylon12/NR] blends.

The tensile yield stress increased with small SEBS content then decreased with increasing content of SEBS. The effect of SEBS-

g-MA content on the tensile stress also showed the same trend as tensile modulus in Figure 4.17.

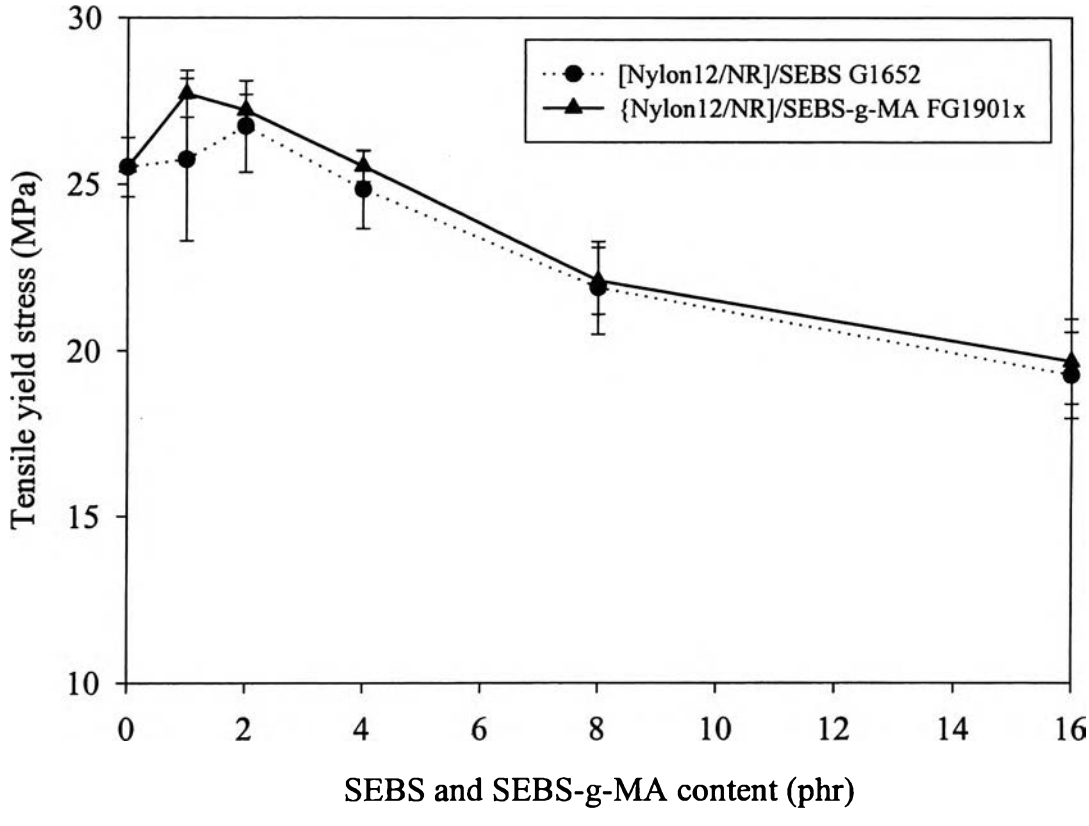

Figure 4.17 Comparison between effect of SEBS-g-MA and SEBS content on tensile yield stress of 80/20 [Nylon12/NR] blends.

4.3.4.5 *Thermal Properties*

The glass transition temperature of Nylon12 in [Nylon12/NR]/SEBS-g-MA blends was increased as increasing SEBS-g-MA in the blends from imide linkage of Nylon12 with SEBS-g-MA. The blends showed the leveling T_m and T_c as increasing SEBS-g-MA content shown in Figure 4.18.

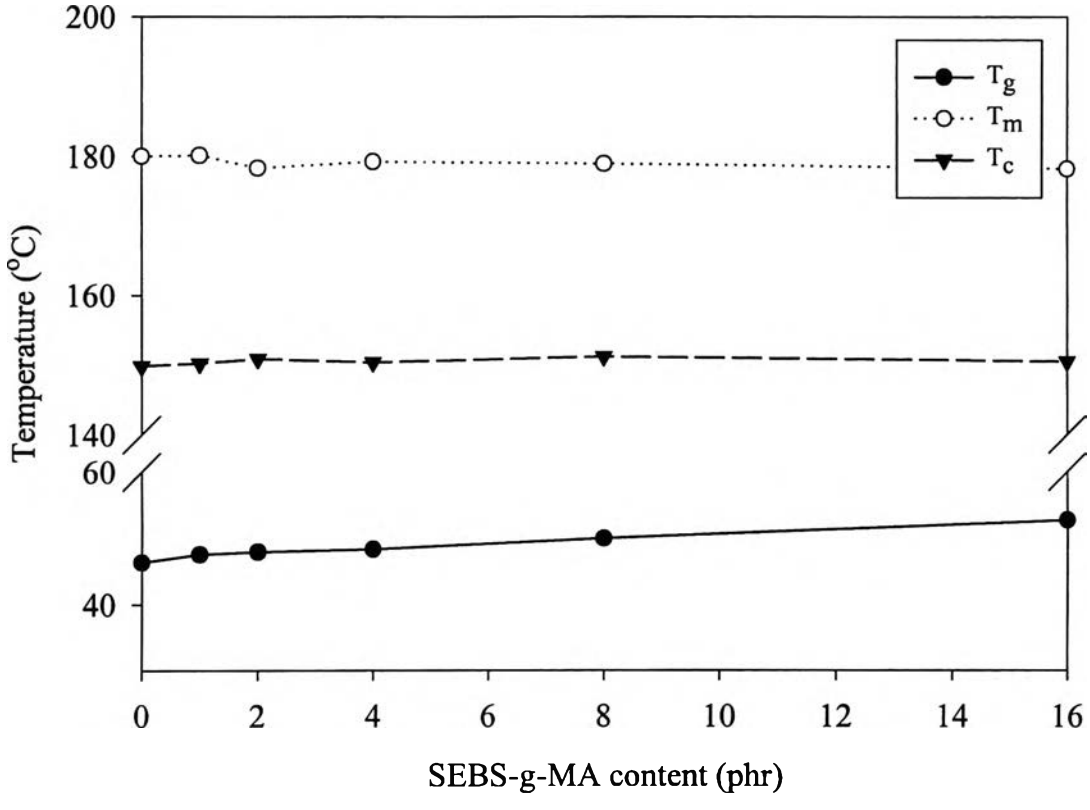

Figure 4.18 T_g, T_m, and T_c of Nylon12 in [Nylon12/NR]/SEBS-g-MA blends with variation of SEBS-g-MA content.

4.3.5 Effect of Molecular Weight of SEBS in Nylon12/NR Blends

4.3.5.1 *Phase Morphology Characterization by TEM*

The phase morphology of [Nylon12/NR]/SEBS G1650 blend was coarser and more heterogeneous than in the [Nylon12/NR]/SEBS G1652 blend. The comparison between [Nylon12/NR]/ SEBS G1650 and [Nylon12/NR]/SEBS G1652 blends at [80/20]/4 phr composition was illustrated in Figure 4.19.

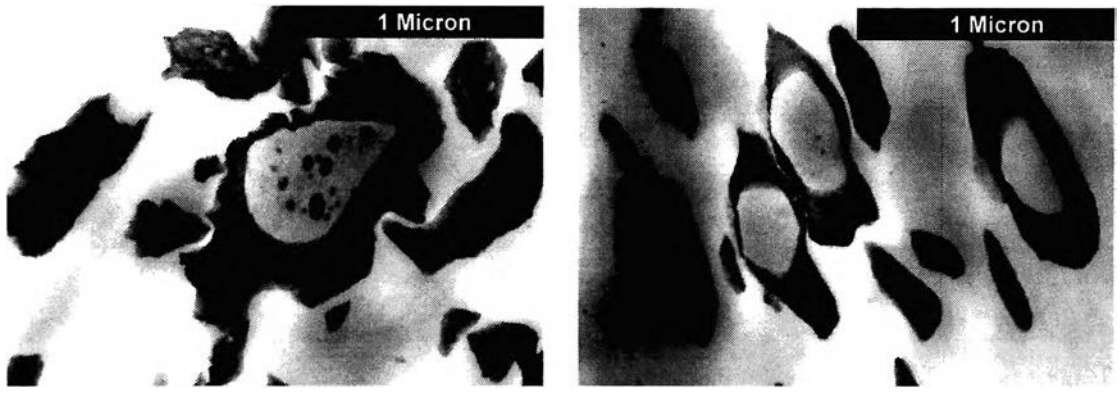

(a) (b)

Figure 4.19 TEM micrographs with a magnification of 55500x of the ultra thin microtomed (a) [80/20]/4phr [Nylon12/NR]SEBS G1650 blend and (b) [80/20]/4phr [Nylon12/NR]/SEBS G1652 blend.

4.3.5.2 *Dispersed Phase Size Characterization by SEM*

Dispersed phase size of [Nylon12/NR]/SEBS G1650 with variation of SEBS content showed the increasing dispersed phase size as increasing SEBS content very similar to that found in the blend with G1652 (Figures 4.20 and 4.21). It was interesting to see that the particle sizes of these blends having SEBS G1650 less than 8 phr were relatively smaller than those of the blends with G1652. This showed the contribution of longer compatibilizer chain to enhance homogeneity, stabilized the interface and morphology and prevent coalescence. When more G1650 was added, the particle size and its distribution increase and was larger than that of G1652.

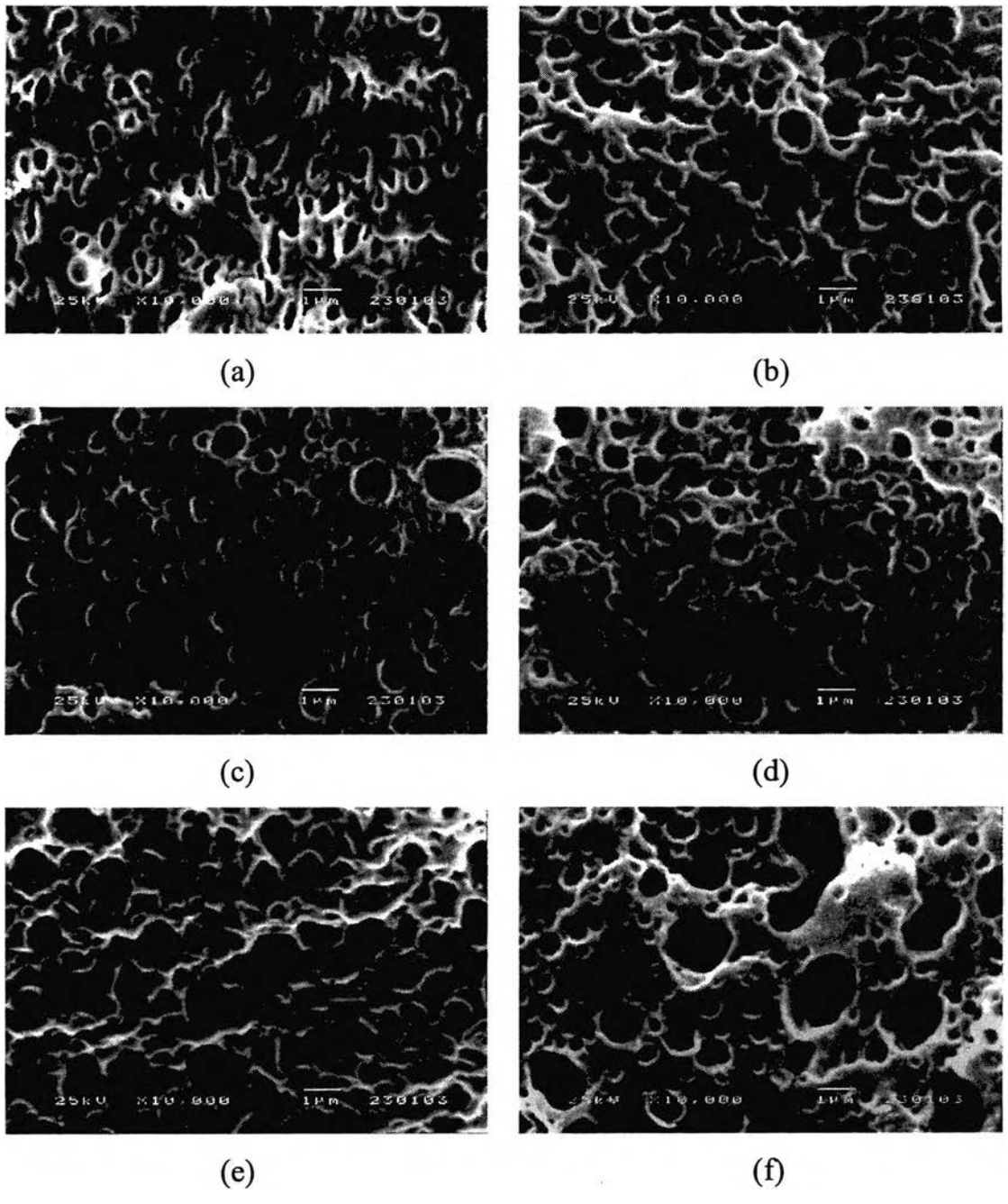

Figure 4.20 SEM micrographs of the cryofracture surfaces of the [80/20] [Nylon12/NR] blends at various SEBS G1650 contents (a) 0 phr, (b) 1 phr, (c) 2 phr, (d) 4 phr, (e) 8 phr, and (f) 16 phr.

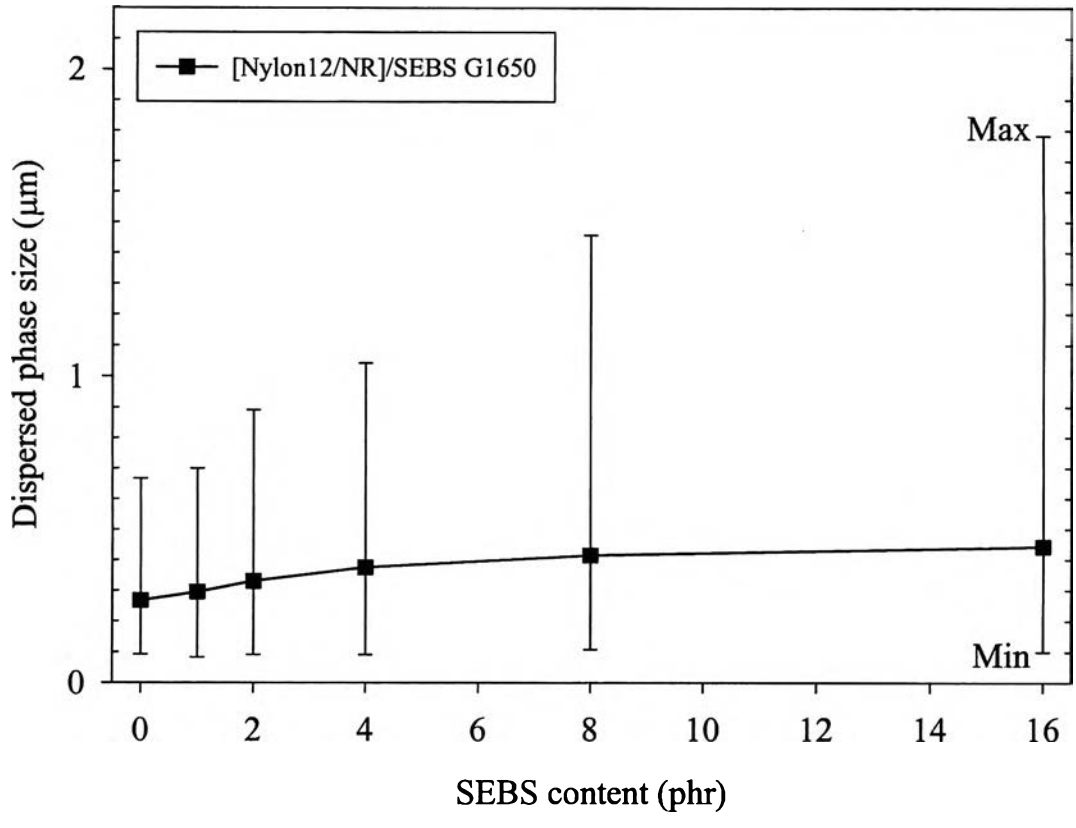

Figure 4.21 Dispersed phase size and distribution of [Nylon12/NR]/SEBS G1650 blends with 0, 1, 2, 4, 8, and 16 phr of SEBS.

4.3.5.3 *Mechanical Properties*

The [Nylon12/NR]/SEBS G1650 showed a slightly higher tensile modulus than [Nylon12/NR]/SEBS G1652 at low content of SEBS, see Figure 4.22. The results corresponded to the decrease in particle size of the blends with G1650 indicating the better adhesion of the two phases due to longer chain of SEBS. However, increasing G1650 content led to an increase in particle size so that the tensile modulus reduced.

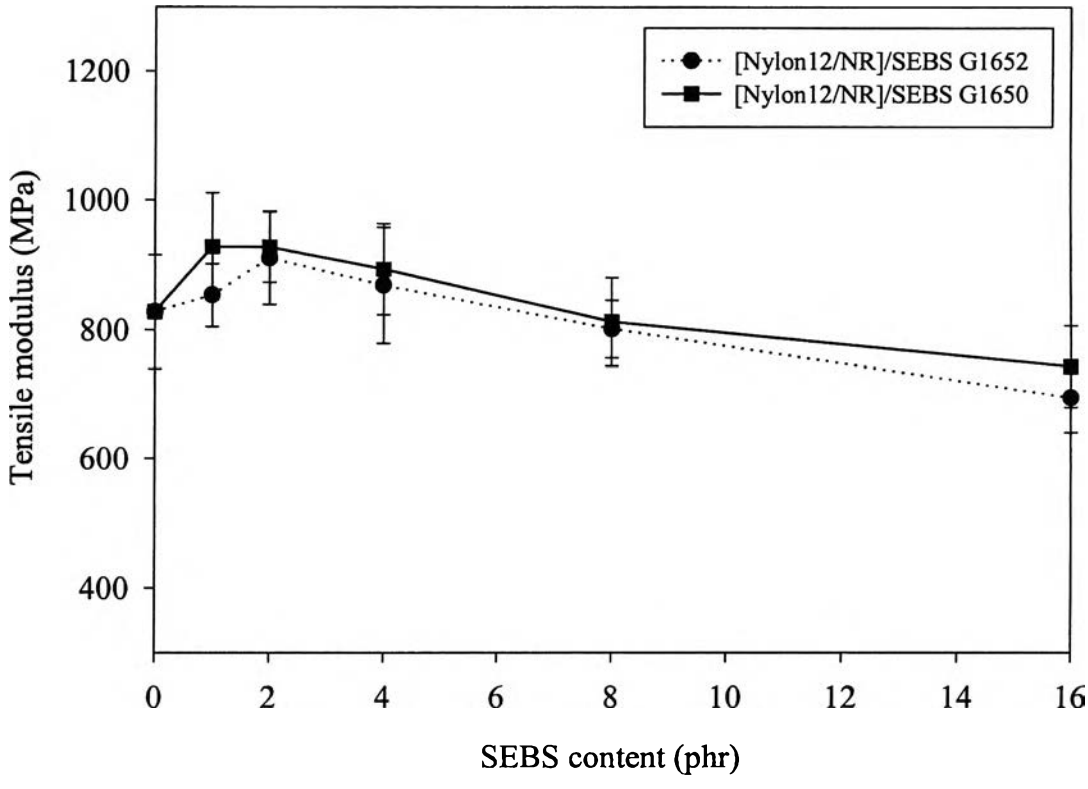

Figure 4.22 Comparison between effect of SEBS G1650 and SEBS G1652 content on tensile modulus of 80/20 [Nylon12/NR] blends.

The tensile yield stress of [Nylon12/NR]/G1650 increased at small SEBS amount then decreased with increasing content of SEBS. The yield values were larger than the blend with G1652. It is inferred that Higher MW of compatibilizer is more effective to enhance adhesion between two phases. The effect of SEBS G1650 phase on the tensile stress was shown the same trend as tensile modulus see Figure 4.23. Although, the increasing MW of the core part could enhance the mechanical strength, it did not seem to highly improve mechanical strength. This could be a result of simultaneously increasing content of soft segment and a wide distribution of the minor phase.

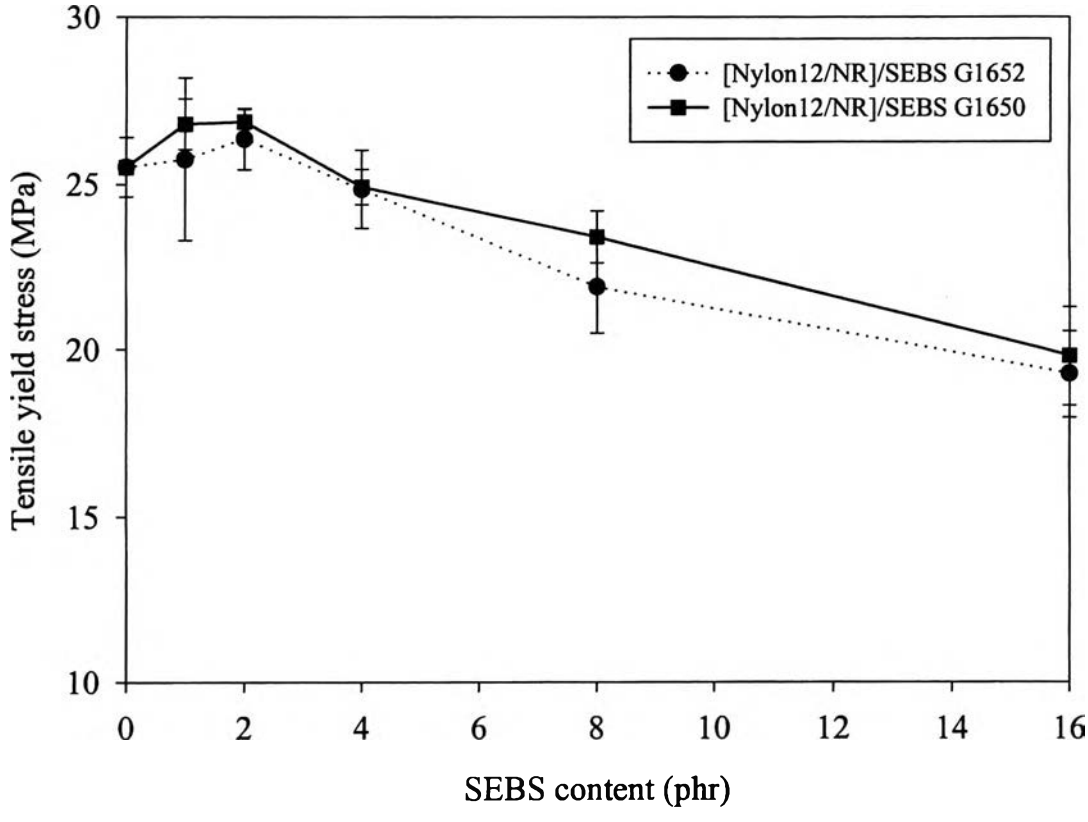

Figure 4.23 Comparison between effect of SEBS G1650 and SEBS G1652 content on tensile yield stress of 80/20 [Nylon12/NR] blends.

4.3.6 Effect of %wt PS of SEBS in Nylon12/NR Blends

4.3.6.1 *Phase Morphology Characterization by TEM*

The [Nylon12/NR]/SEBS G1657 having 13 %wt of PS of SEBS showed the increasing in the size of SEBS core compared with [Nylon12/NR]/SEBS G1650 blend having 30 %wt of PS in Figure 4.24.

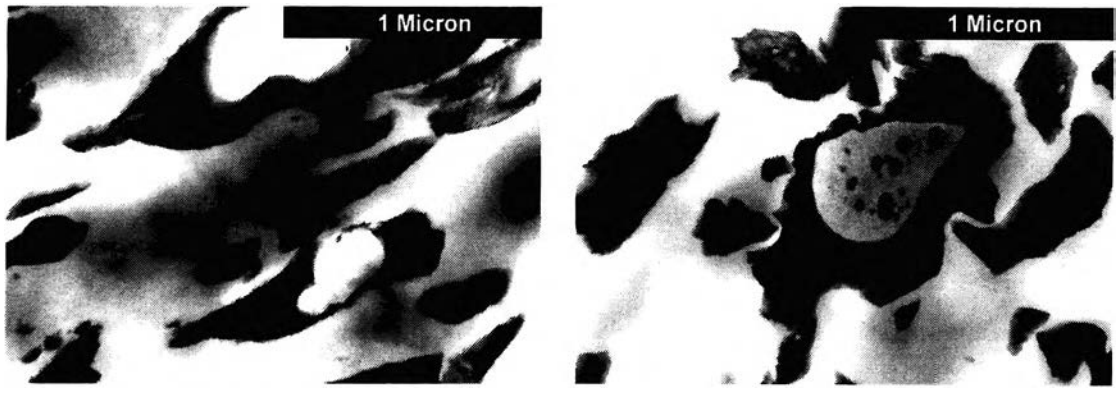

(a) (b)

Figure 4.24 TEM micrographs with a magnification of 55500x of the ultra thin microtomed (a) [80/20]/4phr [Nylon12/NR]SEBS G1657 blend and (b) [80/20]/4phr [Nylon12/NR]/SEBS G1650 blend.

4.3.6.2 *Dispersed Phase Size Characterization by SEM*

The [Nylon12/NR]/SEBS G1657 blends with variation of SEBS content also showed the increasing dispersed phase size with increasing SEBS content increasing as found in blends with G1650, see Figures 4.25and 4.26. The PS core size was obviously reduced with a thick rubber shell as a result of low PS content.

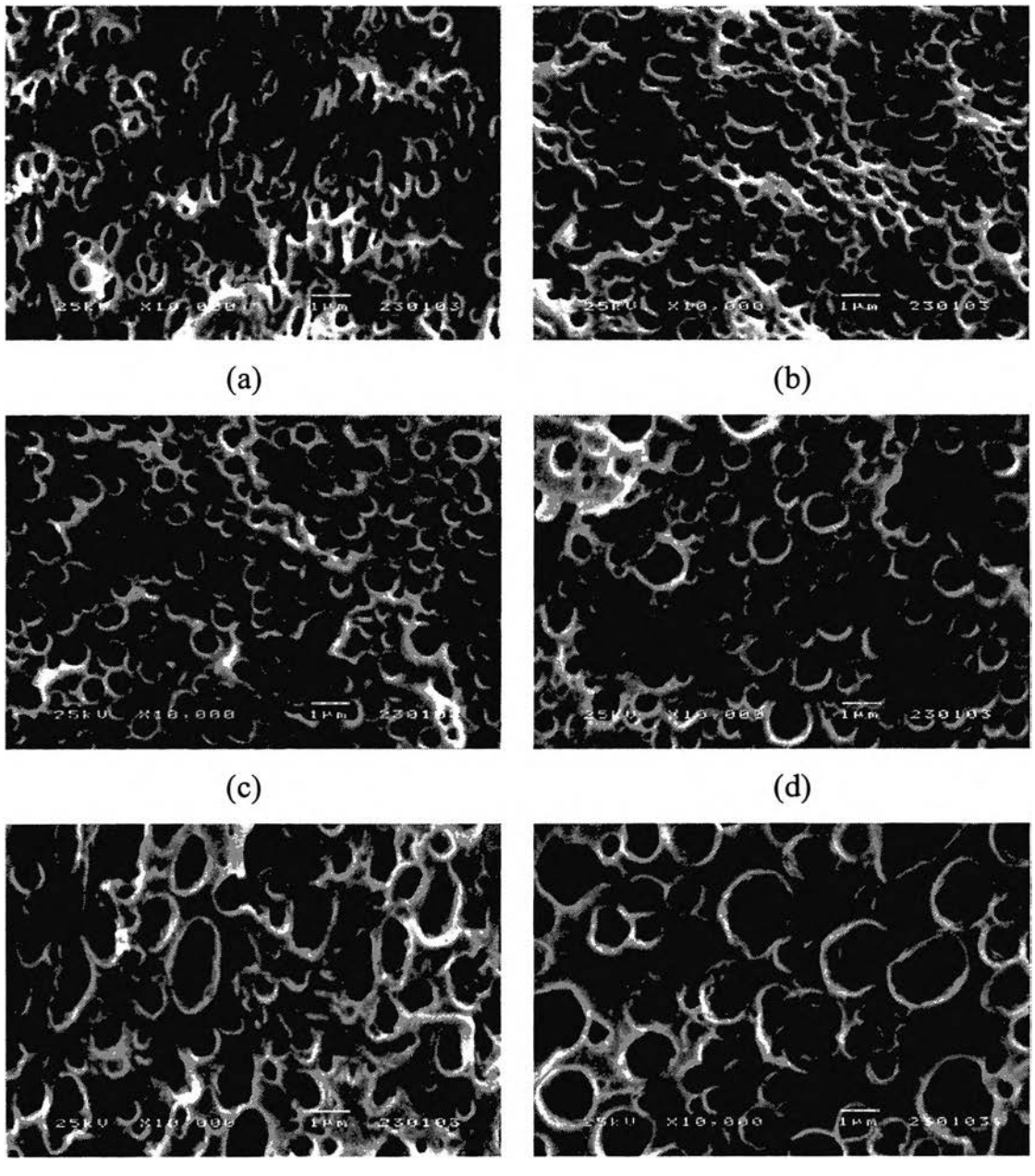

Figure 4.25 SEM micrographs of the cryofracture surfaces of the [80/20] [Nylon12/NR] blends at various SEBS G1657 contents (a) 0 phr, (b) 1 phr, (c) 2 phr, (d) 4 phr, (e) 8 phr, and (f) 16 phr.

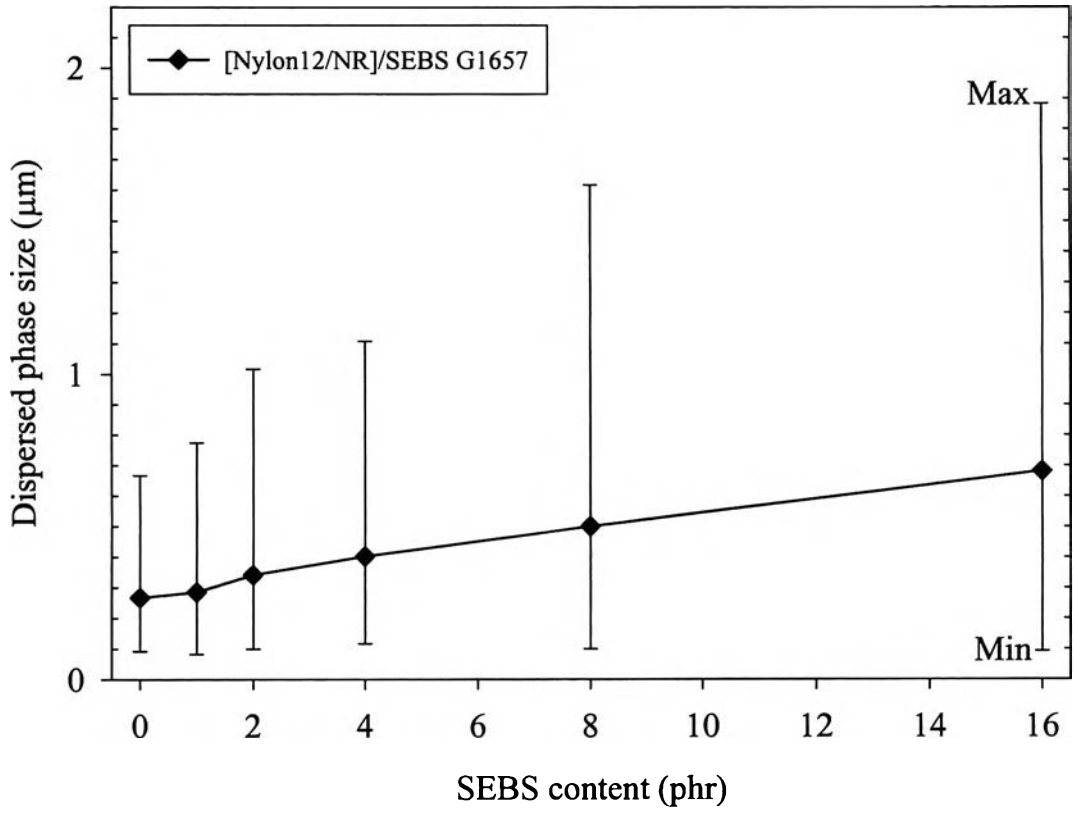

Figure 4.26 Dispersed phase size and distribution of [Nylon12/NR]/ SEBS G1657 blends with 0, 1, 2, 4, 8, and 16 phr of SEBS.

4.3.6.3 *Mechanical Properties*

The [Nylon12/NR]/SEBS G1657 showed slightly lower tensile modulus than in [Nylon12/NR]/SEBS G1650 from the change of %wt of PS from 30 to 13 shown in Figure 4.27. As in Figure 4.27, tensile moduli of both blends were very comparable. This indicated that lowering the content of PS (or increasing EB content) did not significantly decrease the modulus. However, it was obviously affected on tensile yield stress.

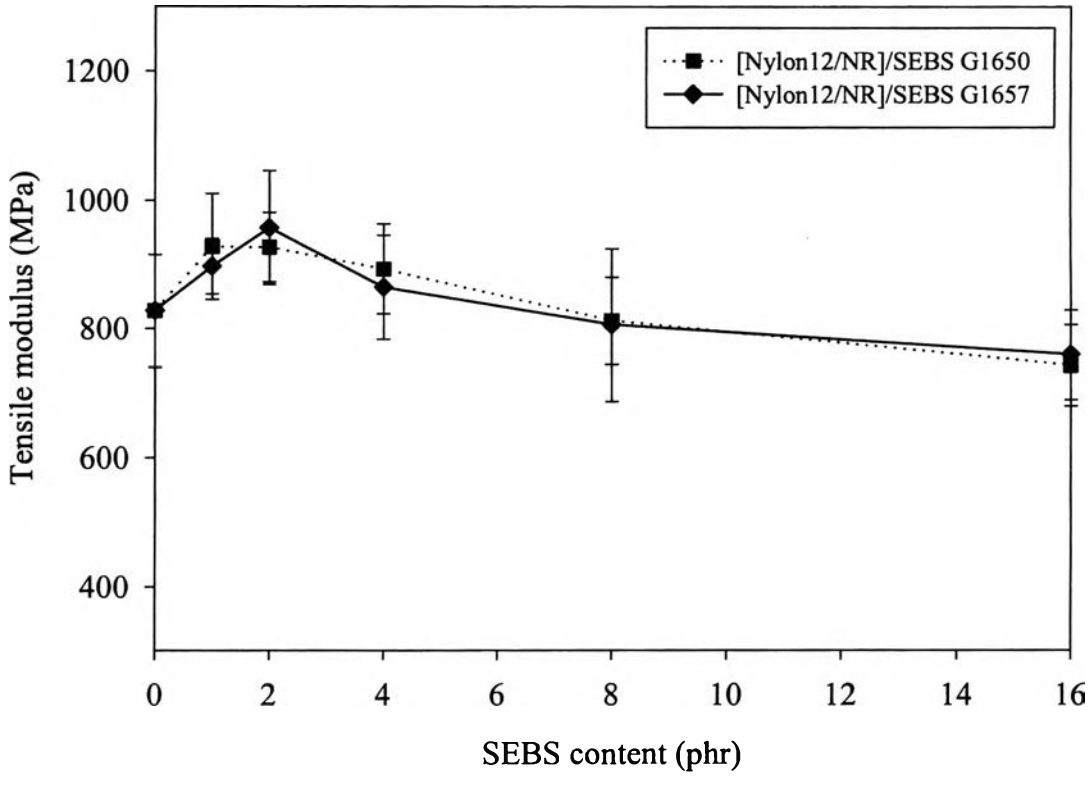

Figure 4.27 Comparison between effect of SEBS G1657 and SEBS G1650 content on tensile modulus of 80/20 [Nylon12/NR] blends.

The [Nylon12/NR]/SEBS G1657 showed the lower tensile stress than [Nylon12/NR]/SEBS G1650 (Figure 4.28). The lower mechanical properties of SEBS G1657 blends corresponded to the shorter PS segments in SEBS. The SEBS is thermoplastic elastomer having PS domains capable to stay together as a hard pseudo-crosslinking point. The lower %PS resulted in smaller PS domains and weaker SEBS type.

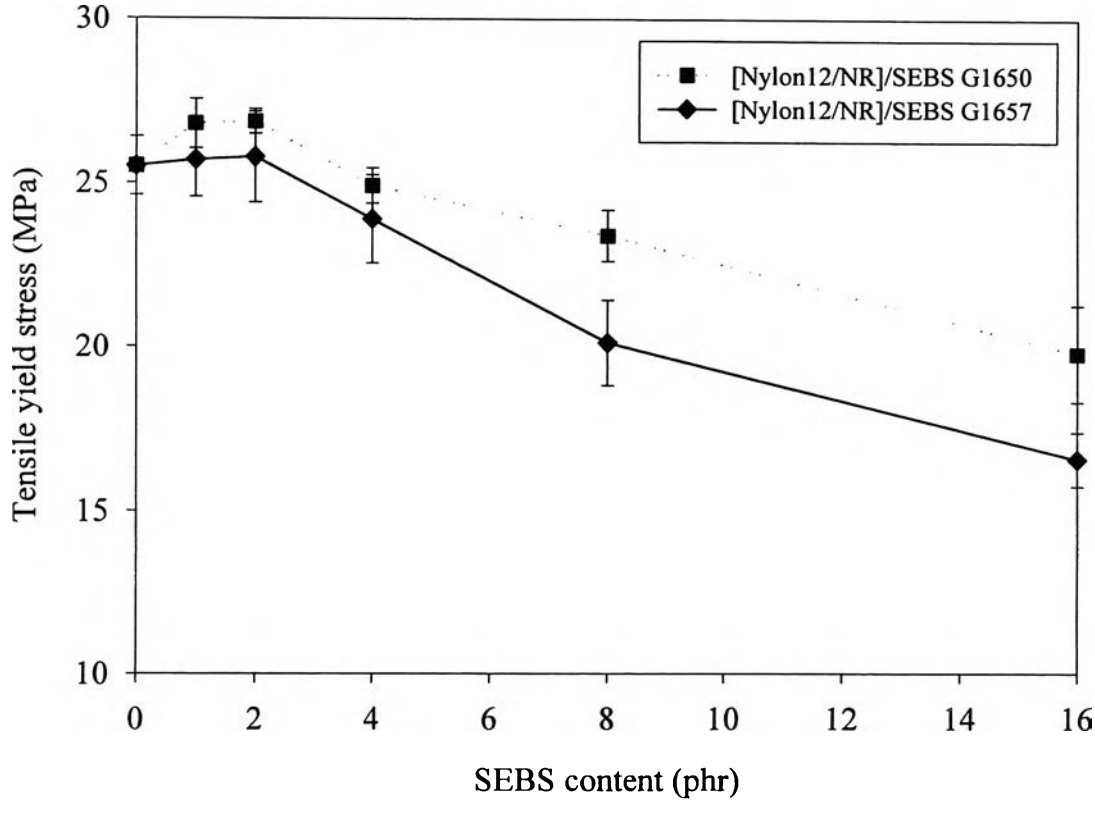

Figure 4.28 Comparison between effect of SEBS G1657 and SEBS G1650 content on tensile yield stress of 80/20 [Nylon12/NR] blends.

4.3.7 Effect of PS/NR with DCP 0.5 phr (PSNR05) Blend in Nylon12/NR Blends

4.3.7.1 *Phase Morphology Characterization by TEM*

Figure 4.29 showed only inclusion of PS (core) in rubber particle (shell) in [Nylon12/NR]/PSNR05 blend compared with the [Nylon12/NR]/SEBS G1650 blend morphology. This should attributed to the excellent compatibility of NR phase in the bulk and in PSNR05.

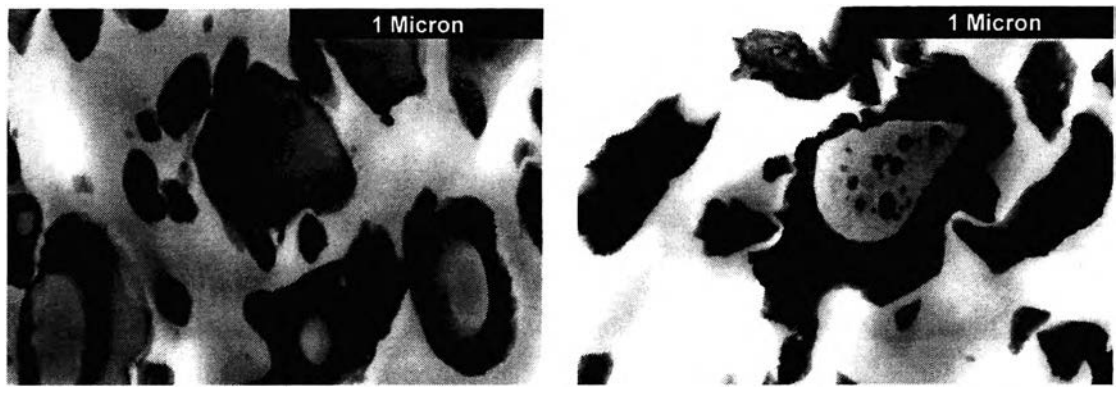

(a) (b)

Figure 4.29 TEM micrographs with a magnification of 55500x of the ultra thin microtomed (a) [80/20]/4phr [Nylon12/NR]SEBS PSNR05 blend and (b) [80/20]/4phr [Nylon12/NR]/SEBS G1650 blend.

4.3.7.2 *Dispersed Phase Size Characterization by SEM*

The [Nylon12/NR]/PSNR05 blends with variation of PSNR05 content showed the increasing dispersed phase size with increasing PSNR05 content in the blends (Figures 4.30 and 4.31). The distribution of the dispersed phase size was the highest.

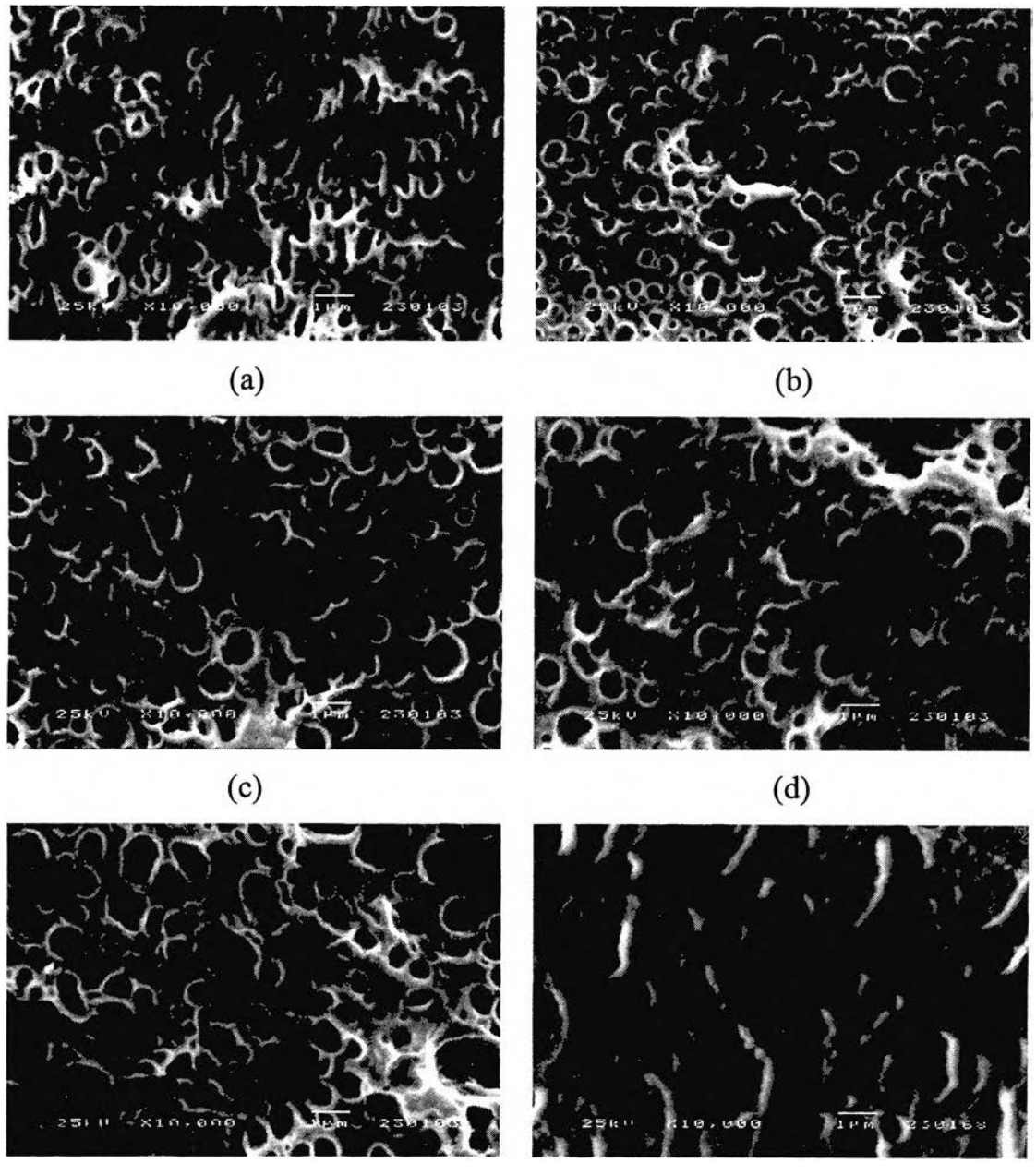

(a) (b)

(c) (d)

(e) (f)

Figure 4.30 SEM micrographs of the cryofracture surfaces of the [80/20] [Nylon12/NR] blends at various PSNR05 contents (a) 0 phr, (b) 1 phr, (c) 2 phr, (d) 4 phr, (e) 8 phr, and (f) 16 phr.

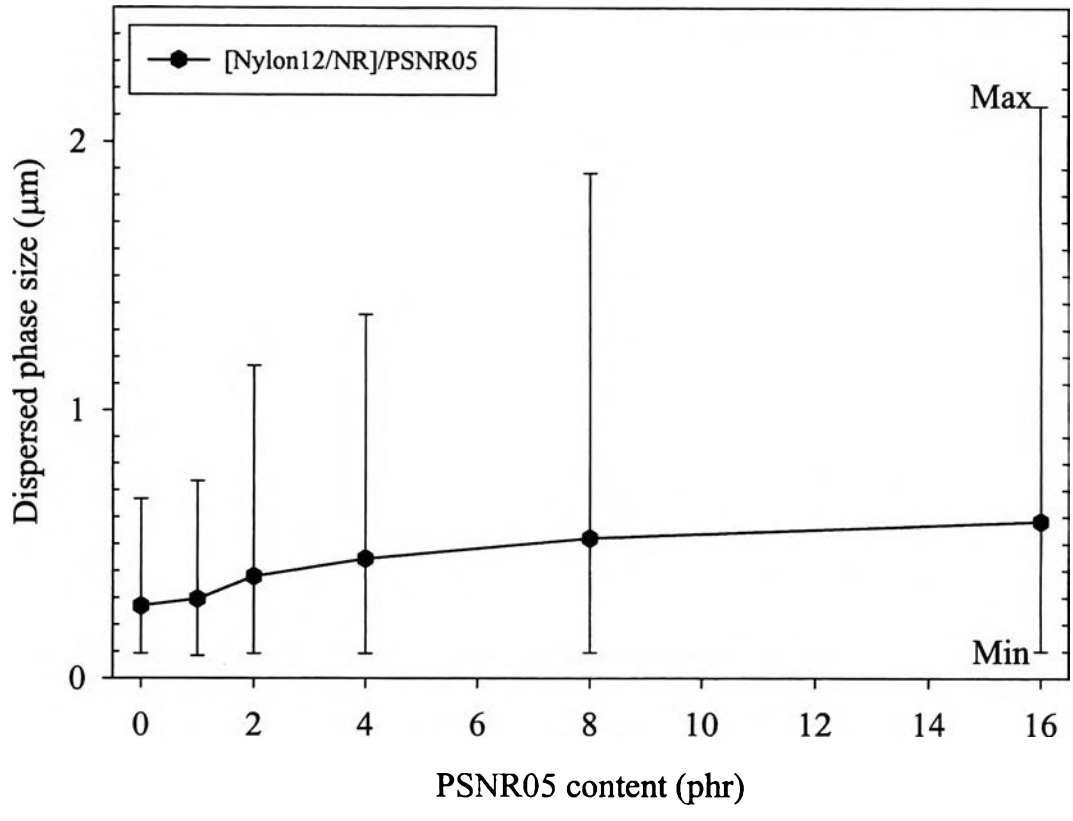

Figure 4.31 Dispersed phase size and distribution of [Nylon12/NR]/ PSNR05 blends with 0, 1, 2, 4, 8, and 16 phr of PSNR05.

4.3.7.3 *Mechanical Properties*

The [Nylon12/NR]/PSNR05 showed a substantially higher tensile modulus than [Nylon12/NR]/SEBS G1650 shown in Figure 4.32. The PSNR05 contained 60%PS which was double the content of PS in SEBS G1650. Thus the content of soft NR phase was significantly reduced. Moreover, there was the crosslinked NR in PSNR05. Consequently, the PS hard segment (60%PS) and NR crosslinking contributed to the higher modulus of this blend compared to the other.

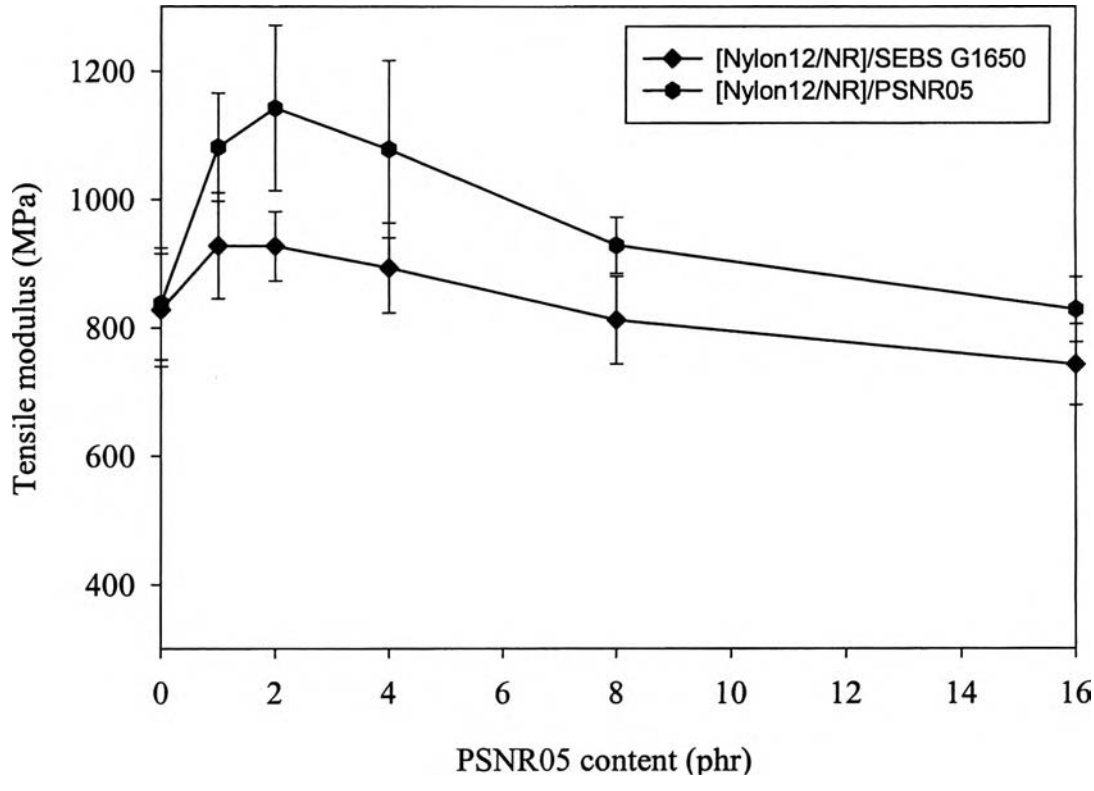

Figure 4.32 Comparison between effect of PSNR05 and SEBS G1650 content on tensile modulus of 80/20 [Nylon12/NR] blends.

The [Nylon12/NR]/PSNR05 showed the comparative strength with those blends with SEBS-g-MA at low PSNR05 content. However, at high PSNR05 content, the tensile yield stress of this blend was lower than that of the blend with G1650, see Figure 4.33. This might be cause by the increasing gel content.

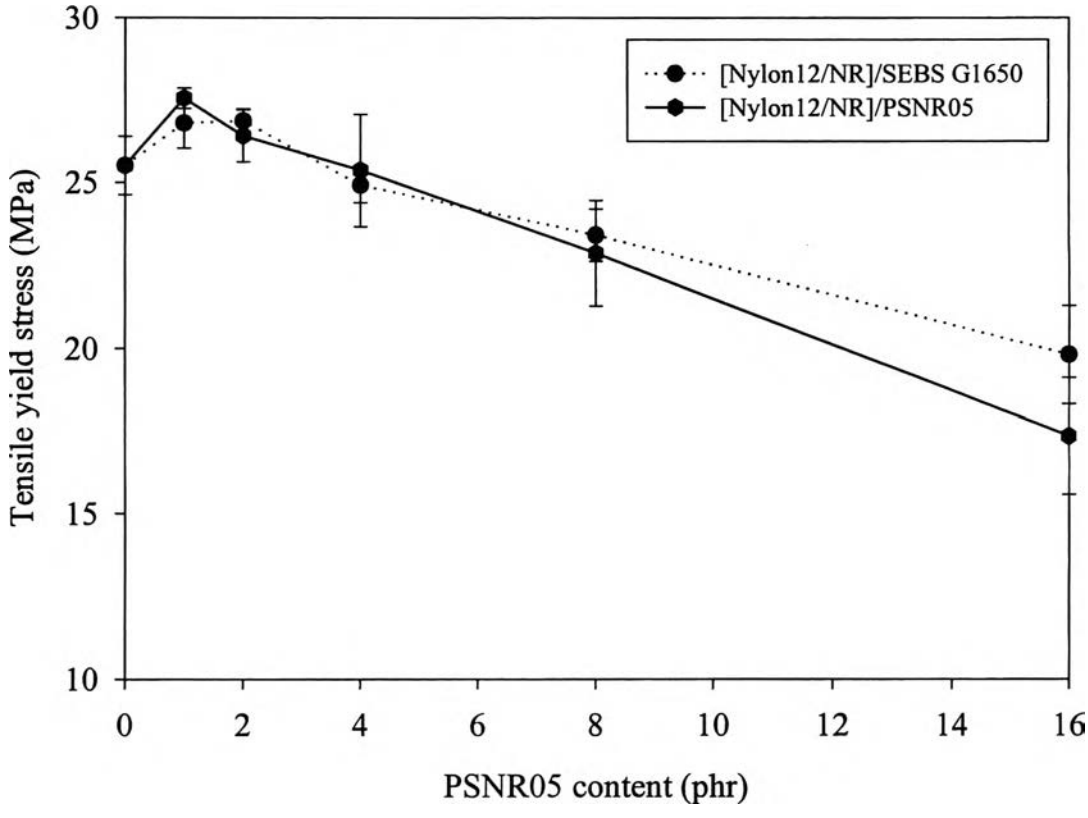

Figure 4.33 Comparison between effect of PSNR05 and SEBS G1650 content on tensile yield stress of 80/20 [Nylon12/NR] blends.

4.3.7.4 *Thermal Properties*

The [Nylon12/NR]/PSNR05 blends also showed the leveling T_g, T_m, and T_c when PSNR05 content increased as the [Nylon12/NR]/SEBS blends (shown in Figure 4.34).

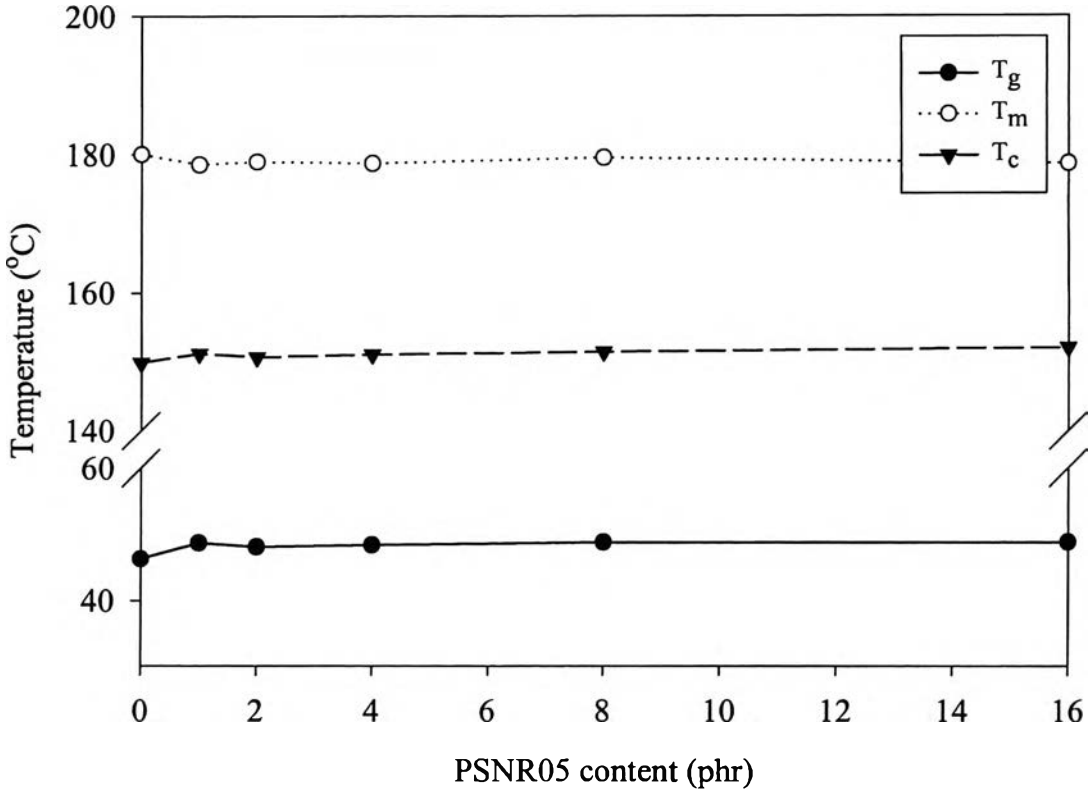

Figure 4.34 T_g, T_m, and T_c of Nylon12 in [Nylon12/NR]/PSNR05 blends with variation of PSNR05 content.

4.3.8 Effect of Various Types and Content of Copolymer on Crystallinity of Nylon12 in Nylon12/NR Blends

The %relative crystallinity of Nylon12 in [Nylon12/NR]/ copolymers observed by DSC were shown in Figure 4.35. Comparing between the blends having SEBS-g-MA FG1901x and SEBS G1652, the [Nylon12/NR]/ SEBS-g-MA showed the higher decreasing crystallinity as increasing SEBS-g-MA content than SEBS and PSNR05 blends because the imide linkage between Nylon12 and SEBS-g-MA and the high dispersion of dispersed phase in Nylon12 matrix obstructed the movement of Nylon12 chains to form the crystal.

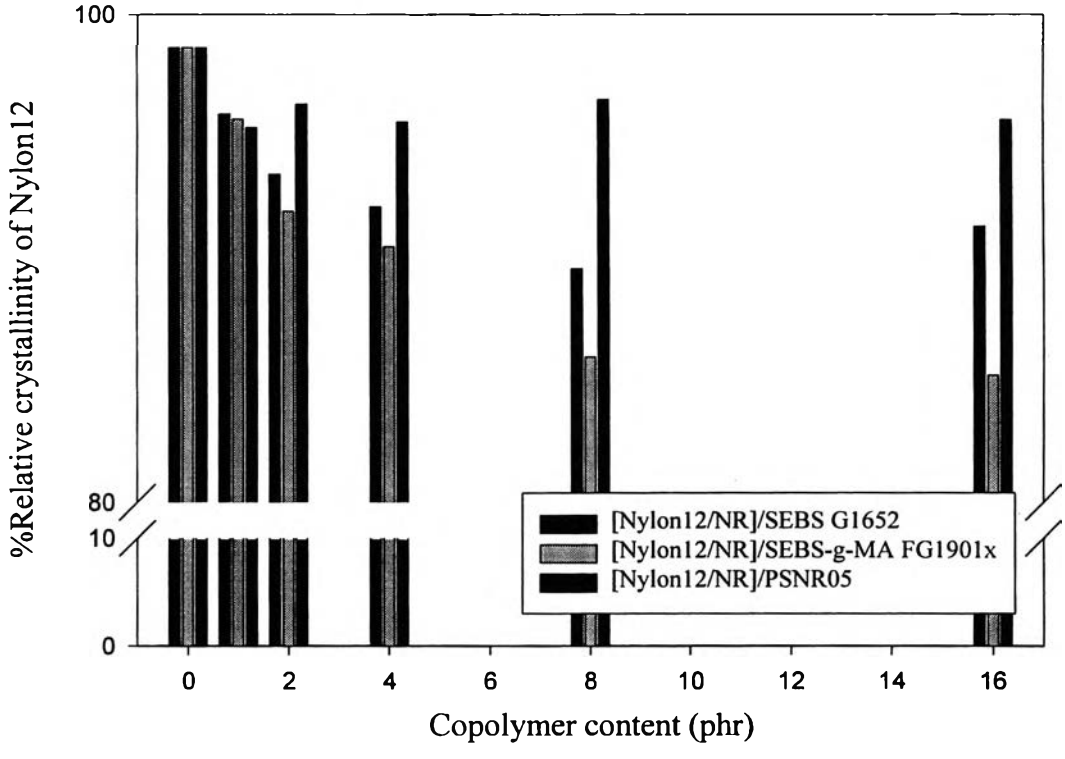

Figure 4.35 %Relative crystallinity of Nylon12 in [Nylon12/NR]/Copolymer blends with variation of copolymer types and content.

It was interesting to see that crystallinity of the blend with PSNR05 was the highest and slightly lower than that of pure Nylon12. The crystallinity did not vary much with PSNR05 and SEBS G1652 (>4phr) but changed largely with SEBS-g-MA FG1901x content.